Eddy Mixing of Potential Vorticity versus Thickness in an Isopycnic Ocean Model

SYBREN S. DRIJFHOUT AND WILCO HAZELEGER

Royal Netherlands Meteorological Institute, De Bilt, Netherlands

(Manuscript received 15 November 1999, in final form 27 April 2000)

ABSTRACT

Parameterizations of the eddy-induced velocity that advects tracers in addition to the Eulerian mean flow are traditionally expressed as a downgradient Fickian diffusion of either isopycnal layer thickness or large-scale potential vorticity (PV). There is an ongoing debate on which of the two closures is better and how the spatial dependence of the eddy diffusivity should look like. To increase the physical reasoning on which these closures are based, the authors present a systematic assessment of eddy fluxes of thickness and PV and their relation to mean-flow gradients in an isopycnic eddy-resolving model of an idealized double-gyre circulation in a flat bottom, closed basin. The simulated flow features strong nonlinearities, such as tight inertial recirculations, a meandering midlatitude jet, pools of homogenized PV, and regions of weak flow where β/h dominates the PV gradient. It is found that the zonally averaged eddy flux of thickness scales better with the zonally averaged meridional thickness gradient than the eddy flux of PV with the PV gradient. The reason for this is that the two-scale approximation, which is often invoked to derive a balance between the downgradient eddy flux of PV and enstrophy dissipation, does not hold. It is obscured by advection of perturbation enstrophy, which is multisigned and weakly related to mean-flow gradients. On the other hand, forcing by vertical motions, which enters the balance between the downgradient eddy flux of thickness and dissipation in most cases, acts to dissipate thickness variance. It is dominated by the conversion from potential to kinetic energy and the subsequent downgradient transport of thickness. Also, advection of perturbation thickness variance tends to be more single-signed than advection of perturbation enstrophy, forcing the eddy flux of thickness to be more often down the mean gradient. As a result, in the present configuration a downgradient diffusive closure for thickness seems more appropriate to simulate the divergent eddy fluxes than a downgradient diffusive closure for PV, especially in dynamically active regions where the eddy fluxes are large and in regions of nearly uniform PV.

1. Introduction

Modeling the ocean circulation implies calculation of a solution to a particular set of equations (e.g., the primitive equations) that describes the motion of the resolved scales, with source/sink terms added that contain parameterizations of the unresolved scales. Until recently, these parameterizations consisted of a diffusion of tracer and momentum along the coordinate directions, with the vertical diffusion much smaller than the horizontal. For most global ocean models the unresolved scales that contain the most energy are the mesoscale eddies. Diffusion of momentum in the horizontal by the eddies is questionable, as part of the momentum transport occurs nonlocally through pressure forces. Also, the eddy momentum transport is often observed to be upgradient (e.g., Schmitz 1977; McWilliams et al. 1978). In an integral sense, however, horizontal momentum diffusion is associated with the enstrophy cascade from larger to smaller scales and should be downgradient. For a downgradient formulation of the eddy transport of tracer exists more support, but here the direction should be aligned with isopycnals instead of the coordinate directions in nonisopycnic coordinate models.

The notion that eddies provide an advective transport of tracers in the atmosphere (e.g., Andrews et al. 1987; Plumb and Mahlman 1987) preceded oceanographic approaches. In the oceanographic literature, Gent and McWilliams (1990) and Gent et al. (1995) were the first to show that an additional advection of tracers arises from the correlation of the eddy components of layer thickness and velocity, which then defines a bolus or eddy-induced transport velocity. The Gent and McWilliams scheme has been implemented successfully in coarse-resolution models. For instance, Danabasoglu and McWilliams (1995) and Hirst and McDougall (1996) show that the simulated water mass distribution improves significantly when the scheme is applied. Also, more tentative results have been reported (Duffy et al. 1995; England 1995). Later, the relation between the eddy-induced advection and eddy quantities has been refined by McDougall and McIntosh (1996) and McDougall (1998), and a link with the residual-mean

Corresponding author address: Sybren S. Drijfhout, Royal Netherlands Meteorological Institute (KNMI), P.O. Box 201, 3730 AE, De Bilt, Netherlands.
E-mail: drijfhou@knmi.nl

theory of Andrews and McIntyre (1976) was established. A parameterization of the eddy-induced advection is then established if it is expressed in mean field quantities. Gent and McWilliams (1990) favored a downgradient Fickian diffusion of isopycnal layer thickness. This was motivated as to mimic the domain-averaged effect of baroclinic instability. It provides a negative definite sink of large-scale potential energy, which is assumed to be converted into eddy energy and subsequent frictional losses. Further developments along this line have been given by, for example, Visbeck et al. (1997).

An alternative proposal relating eddy-induced transport to potential vorticity (PV) gradients has been advocated by, for example, Treguier et al. (1997), Lee et al. (1997), and Killworth (1997). Here, the argument is that PV is conserved by fluid particles in an ideal fluid, while layer thickness is not. As a result, in a steady state the divergence of the eddy PV flux will be balanced by the advection by the mean flow of the mean PV gradients. Also, under certain scaling assumptions, in the equation for perturbation enstrophy the cross-gradient eddy flux of PV is balanced by dissipation and at most places both terms should be negative. This suggests that a diffusive closure in PV should work better than in the case of layer thickness transports.

A host of arguments exists pro or contra one of these closures. For instance, PV is observed to be homogenized within gyres on subsurface isopycnal surfaces (McDowell et al. 1982; O'Dwyer and Williams 1997). A closure of the eddy PV flux can form the basis for a closure of the eddy momentum transport (Greatbatch 1998). It is observed to perform better than an eddy layer-thickness flux closure in channel models (Lee et al. 1997; Treguier 1999; Marshall et al. 1999). Against this it can be argued that the ocean is not an ideal fluid, that closures based on PV mixing appear to be singular at the equator (the quasigeostrophic approximation has to be valid). The role of eddy fluxes in a gyre circulation where zonal asymmetries exist is completely different from those in channel models (Rhines and Holland 1979; Holland and Rhines 1980). The spatial inhomogeneity of eddy momentum transport causes the eddy flux of relative vorticity to be small scale and seemingly unrelated to the large-scale PV gradient (Holland and Rhines 1980).

In the present study we aim at improving the physical reasoning on which the closures for eddy fluxes previously discussed are based. To this end, we perform a systematic assessment of eddy fluxes and their relation to mean flow gradients in an isopycnic eddy-resolving model of an idealized double-gyre circulation in a flat bottom, closed basin. Before evaluating the eddy fluxes we decompose them into a rotational and divergent part. In zonal averages of meridional fluxes in a periodic channel flow, the rotational part of the flow vanishes. In that case, one may diagnose the eddy-induced transfer velocity itself and compare it with the parameterizations [this has been done by, e.g., Lee et al. (1997)]. In a closed basin the rotational fluxes do not vanish and may even dominate the divergent fluxes (Marshall and Shutts 1981). As only the divergent component of the flux contributes to the divergence of the eddy transports, it is only this part that needs to be parameterized.

This study emphasizes flow with moderately high Reynolds numbers (i.e., the basinwide variation in upper-layer depth is of the order of the average layer depth itself, but outcropping does not occur) for which the quasigeostrophic assumption may not be valid in the western boundary currents and midlatitude jet. As eddy fluxes tend to peak where the variability is high (Stammer 1998; Wunsch 1999), we feel that it is pertinent to test these closure schemes where we expect them to be most important. A corrolary of this model configuration is that much of the physical reasoning used in the studies discussed above may no longer be valid, as they are (partly) based on assumptions and approximations that do not hold for this type of flow. In the present paper we emphasize the more fundamental aspects of eddy mixing of PV and isopycnal layer thickness by highlighting the processes that cause well-, or less well-behaved downgradient eddy transports. In a companion paper we will address the spatial structure of the effective eddy diffusivity and test the performance of several closure schemes in a coarse-resolution model.

This paper is organized as follows. In section 2 we review briefly the theoretical framework. In section 3 we address the model formulation, the forcing, and the mean fields. In section 4 the eddy transports are decomposed into rotational and divergent parts, and from the latter the cross-gradient and along-gradient properties are discussed. Next, we evaluate the zonally averaged flux-gradient relations (section 5) and discuss the physics that cause departures from simple Fickian downgradient diffusion (section 6). Finally, in section 7 the conclusions are given.

2. Theoretical background

In this section we review briefly the problem of eddy parameterization. An incompressible, adiabatic, Boussinesq flow in isopycnal coordinates is considered. When a layer formulation is used (i.e., homogeneous layers of constant density), the vertical integral of the continuity equation between two isopycnal surfaces results in a layer thickness equation:

$$\frac{\partial h}{\partial t} + \nabla \cdot (\mathbf{u}h) = 0, \tag{1}$$

with $\mathbf{u} = (u, v)$ the horizontal velocity and h the layer thickness. Similarly, for a tracer τ we can write

$$\frac{\partial (h\tau)}{\partial t} + \nabla \cdot (\mathbf{u}h\tau) = 0. \tag{2}$$

In coarse-resolution ocean models, only the large-scale

mean flow is resolved. In order to study the effect of the unresolved eddies we define a time mean (averaged over several eddy cycles, denoted by an overbar) and an eddy part that is the departure from the mean (denoted by a prime) of the flow. This results in the following equations for the mean thickness:

$$\frac{\partial \overline{h}}{\partial t} + \nabla \cdot (\overline{\mathbf{u}}\,\overline{h} + \overline{\mathbf{u}'h'}) = 0, \tag{3}$$

and for tracer:

$$\frac{\partial(\overline{h}\,\overline{\tau} + \overline{h'\tau'})}{\partial t} + \nabla \cdot (\overline{\mathbf{u}}\,\overline{h}\,\overline{\tau} + \overline{\mathbf{u}'h'}\,\overline{\tau}) = -\nabla \cdot [\overline{(\mathbf{u}h)'\tau'}]. \tag{4}$$

From these equations the time mean tracer equation can be derived (Gent et al. 1995):

$$\frac{\partial \overline{\tau}}{\partial t} + (\overline{\mathbf{u}} + \mathbf{u}_*) \cdot \nabla \overline{\tau} = \nabla \cdot (\kappa \overline{h} \nabla \overline{\tau})/\overline{h}, \tag{5}$$

and equivalently for thickness,

$$\frac{\partial \overline{h}}{\partial t} + \nabla \cdot [\overline{h}(\overline{\mathbf{u}} + \mathbf{u}_*)] = 0. \tag{6}$$

Here, $\mathbf{u}_* = \overline{\mathbf{u}'h'}/\overline{h}$ is an eddy-induced advection term, often called the bolus velocity. So, there is an eddy-induced transport $\overline{\mathbf{u}'h'}$ in addition to the mean transport $\overline{\mathbf{u}}\overline{h}$. In deriving Eq. (5) it is assumed that the eddy correlation between thickness and tracer is small and that

$$-\nabla \cdot [\overline{(\mathbf{u}h)'\tau'}]/\overline{h} = \nabla \cdot (\kappa \overline{h} \nabla \overline{\tau})/\overline{h}. \tag{7}$$

Now, the bolus velocity $\mathbf{u}_*$ can be parameterized assuming downgradient diffusion of layer thickness by the eddy fluxes (Gent et al. 1995; Visbeck et al. 1997), from which it immediately follows that

$$\mathbf{u}_* = -\frac{\kappa_h}{\overline{h}} \nabla \overline{h}. \tag{8}$$

Also, the bolus velocity $\mathbf{u}_*$ can be parameterized assuming downgradient diffusion of PV by the eddy fluxes (Treguier et al. 1997; Lee et al. 1997):

$$\overline{\mathbf{u}'q'} = -\kappa_q \nabla \overline{q}. \tag{9}$$

If, in addition, it is assumed that PV (q) can be approximated by f/h, Eq. (9), becomes

$$\frac{-f\overline{\mathbf{u}'h'}}{\overline{h}^2} = \kappa_q \left[\frac{f \nabla \overline{h}}{\overline{h}^2} - \frac{\nabla f}{\overline{h}} \right]. \tag{10}$$

From the definition of $\mathbf{u}_*$, $\mathbf{u}_* = \overline{\mathbf{u}'h'}/\overline{h}$, it follows that $\mathbf{u}_*$ becomes

$$\mathbf{u}_* = -\frac{\kappa_q}{\overline{h}} \left(\nabla \overline{h} - \frac{\overline{h} \nabla f}{f} \right). \tag{11}$$

Arguments for the downgradient diffusion of the eddy fluxes can be derived from the equations for the perturbation (potential) enstrophy $\overline{q'^2}$ and perturbation thickness variance $\overline{h'^2}$. In steady state, the perturbation enstrophy equation becomes (Rhines and Holland 1979; Treguier et al. 1997)

$$\overline{\mathbf{u}'q'} \cdot \nabla \overline{q} = -\overline{D'_q q'} - \overline{F'_q q'} - \overline{\mathbf{u}} \cdot \frac{\nabla \overline{q'^2}}{2} - \frac{\nabla \cdot \overline{\mathbf{u}'q'^2}}{2}. \tag{12}$$

Here F_q is the forcing of PV and D_q the dissipation. With a constant wind stress $\overline{F'_q q'}$ will be small (F'_q arising from variations in upper-layer depth). The advection of eddy variance by the mean flow and the self-advection of eddy variance are assumed to be $O(\gamma_q)$, or smaller (Rhines and Holland 1979). Here, γ_q is the ratio of particle displacement to the length scale of the q field. Then for γ_q smaller than one, Eq. (12) can be written as

$$\overline{\mathbf{u}'q'} \cdot \nabla \overline{q} = -\overline{D'_q q'} + O(\gamma_q). \tag{13}$$

When the dissipation D_q consists of biharmonic friction, it is not guaranteed that $\overline{D'_q q'}$ is positive, although the basin-integrated sum of this term should be. Rhines and Holland (1979) remark, that when friction acts to dissipate relative vorticity with no, or much less, attendant dissipation of thickness perturbations, in a state of minimum potential enstrophy friction can increase the potential enstrophy. We note here that dissipation of relative vorticity will tend to dominate dissipation of thickness perturbations. Likewise as in all ocean models the diffusion of horizontal momentum, or relative vorticity, is chosen to be larger than the diffusion of tracer, or layer thickness. The domination of relative vorticity dissipation over dissipation of thickness perturbations will be more severe in places where the Reynolds number is large; the western boundary currents and midlatitude jets, exactly those places where the eddy fluxes tend to be the largest. Moreover, in these places the spatial scale of the q field becomes small and γ_q becomes large: $O(1)$. The spatial scale of the q field is now set by the width of the jet and boundary currents. As the relative vorticity becomes more important, the scale of the q field becomes even smaller. So, in regions of high eddy fluxes the assumptions that support a downgradient eddy transport of PV are not valid and a downgradient, diffusive closure becomes questionable.

In steady state, the equation for perturbation thickness variance becomes (Holland and Rhines 1980):

$$\overline{\mathbf{u}'h'} \cdot \nabla \overline{h} = -\overline{D'_h h'} - \overline{w'h'} - \overline{\mathbf{u}} \cdot \frac{\nabla \overline{h'^2}}{2} - \frac{\nabla \cdot \overline{\mathbf{u}'h'^2}}{2}. \tag{14}$$

Here D_h is the dissipation of layer thickness anomalies, and $w' = (h\nabla \cdot \mathbf{u})'$. The advection of eddy variance by the mean flow and the self-advection of eddy variance are now assumed to be $O(\gamma_h)$, or smaller, where γ_h is the ratio of particle displacement to the length scale of the h field. The term $\overline{w'h'}$ appears in Eq. (14), while an equivalent term is absent in Eq. (12) because q is

conserved; $dq/dt = 0$, and h is not conserved; $dh/dt = -h\nabla \cdot \mathbf{u}$. Equation (14) can also be written as

$$\overline{\mathbf{u}'h'} \cdot \nabla \overline{h} = -\overline{D_h'h'} - \overline{w'h'} + O(\gamma_h). \quad (15)$$

We note that $\overline{D_h'h'}$ will more often tend to be positive than $\overline{D_q'q'}$, as the latter consists of possible competing effects between relative vorticity dissipation and dissipation of thickness perturbations. On the other hand, the term $\overline{w'h'}$ complicates the interpretation of Eq. (15). Holland and Rhines (1980) note, however, that this term, being a conversion from potential to kinetic energy, is often associated with downgradient eddy heat transport. Subsequently, $\overline{w'h'}$ tends to be positive when baroclinic instability dominates. It tends to be negative in regions where eddies return energy to the mean flow. In general, the regions where $\overline{w'h'}$ are positive, dominate. Also, the spatial scale of the h field tends to be larger than the scale of the q field in those places where they both become small: the western boundary currents and midlatitude jets. As a consequence, in those places γ_q will go quicker to one than γ_h. So beforehand, we cannot anticipate whether a downgradient transport of PV by the eddies is a more robust feature of the flow and occurs on larger spatial scales than a downgradient transport of layer thickness. We will use a numerical eddy-resolving model to answer this question by investigating the balance in Eqs. (12) and Eq. (14).

3. The model experiment

a. Model formulation

We use a three-layer isopycnal primitive equation model. The model is based on the code of Bleck and Boudra (1986). The domain of the model is rectangular (2500 km × 2500 km), and the bottom is flat (depth is 4000 m). The horizontal resolution is 10 km. The reduced gravity at the layer interfaces is $g_1' = 0.012$ m s^{-2}, $g_2' = 0.014$ m s^{-2}. The mean layer thicknesses are $h_1 = 625$ m, $h_2 = 450$ m, and $h_3 = 2925$ m. The present upper-layer thickness, together with the applied wind forcing, allows for depth variations of the order the average layer thickness, but outcropping is prevented. This enables us to study a flow regime that is no longer constrained by the quasigeostrophic approximation, while singularities associated with outcropping are prevented, as they are connected to diabatically forced flows for which the eddy closures we discuss here are not intended.

In the model a momentum and a layer thickness equation are solved for both layers. The layer integrated horizontal momentum equations are ($n = 1, 2, 3$)

$$\frac{\partial \mathbf{u}_n}{\partial t} + \nabla \cdot \frac{\mathbf{u}_n^2}{2} + (\zeta_n + f)\mathbf{k} \times \mathbf{u}_n = -\nabla M_n - \frac{1}{h_n}\nabla^2 \cdot (A_M h_n \nabla^2 \mathbf{u}_n) + \frac{g}{h_{1,3}}\Delta\tau. \quad (16)$$

Here $\nabla = \partial/\partial x + \partial/\partial y$, $\mathbf{u} = (u, v)$ is the horizontal velocity, $\zeta = \partial v/\partial x - \partial u/\partial y$ is the vertical component of the relative vorticity, $\mathbf{k}$ is the vertical unit vector, $M = gz + p\alpha$ is the Montgomery potential ($\alpha = 1/\rho$ is the specific volume, p is the pressure on the isopycnic surface, z is the depth of the interface of the isopycnic surface), g is the gravity acceleration, A_M is the lateral eddy viscosity parameter, h is the layer thickness, and $\tau = (\tau_x, \tau_y)$ are the wind and bottom-drag-related viscous stresses. A quadratic drag relation parameterizes the bottom drag with a drag coefficient $C_D = 0.003$. It is applied to the lower 25 m of the ocean. A classical cosine zonal wind stress is used with a maximum amplitude of 1.5×10^{-1} N m^{-2}. With this forcing and basin geometry a double-gyre circulation is simulated. The continuity equation is applied to the vertically homogeneous layers. This results in a layer thickness equation:

$$\frac{\partial h_n}{\partial t} + \nabla \cdot (\mathbf{u}_n h_n) = -A_h \nabla^4 h_n. \quad (17)$$

The terms on the left-hand side arise from the adiabatic continuity equation. The third term is the lateral diffusion, which parameterizes subgrid-scale processes (lateral mixing); A_h is the isopycnal diffusivity. The lateral diffusion is 5×10^9 m^4 s^{-1}. The lateral viscosity has a minimum background value of 5×10^9 m^4 s^{-1}, but otherwise scales with the absolute value of the total deformation of the horizontal flow field (Smagorinsky 1963; Bleck and Boudra 1981). The model equations are complemented by a hydrostatic balance (p is the pressure on the isopycnic surface):

$$\frac{\partial M_n}{\partial \alpha} = p_n. \quad (18)$$

Lateral boundary conditions are free slip and a zero flux for all quantities. For more details on the model description we refer to Bleck and Boudra (1986) and Drijfhout (1994).

b. General characteristics

The model has been spun up for 30 years at a resolution of 25 km. Then, the model fields were interpolated to the 10-km horizontal grid size and the model was run for another 22 yr. Data from the last 10 years are used in the following sections.

In Fig. 1 the average barotropic streamfunction together with the layer-integrated streamfunctions for the nondivergent flow in each layer are shown. The streamfunctions show that the model simulates strong western boundary currents, a midlatitude jet, and tight recirculation cells around the jet. The maximum barotropic transport is 65 Sv (Sv $\equiv 10^6$ m^3 s^{-1}). We note that the circulation is far more asymmetric compared to the familiar double-gyre flows in quasigeostrophic models (Holland and Rhines 1980; Holland et al. 1984). The

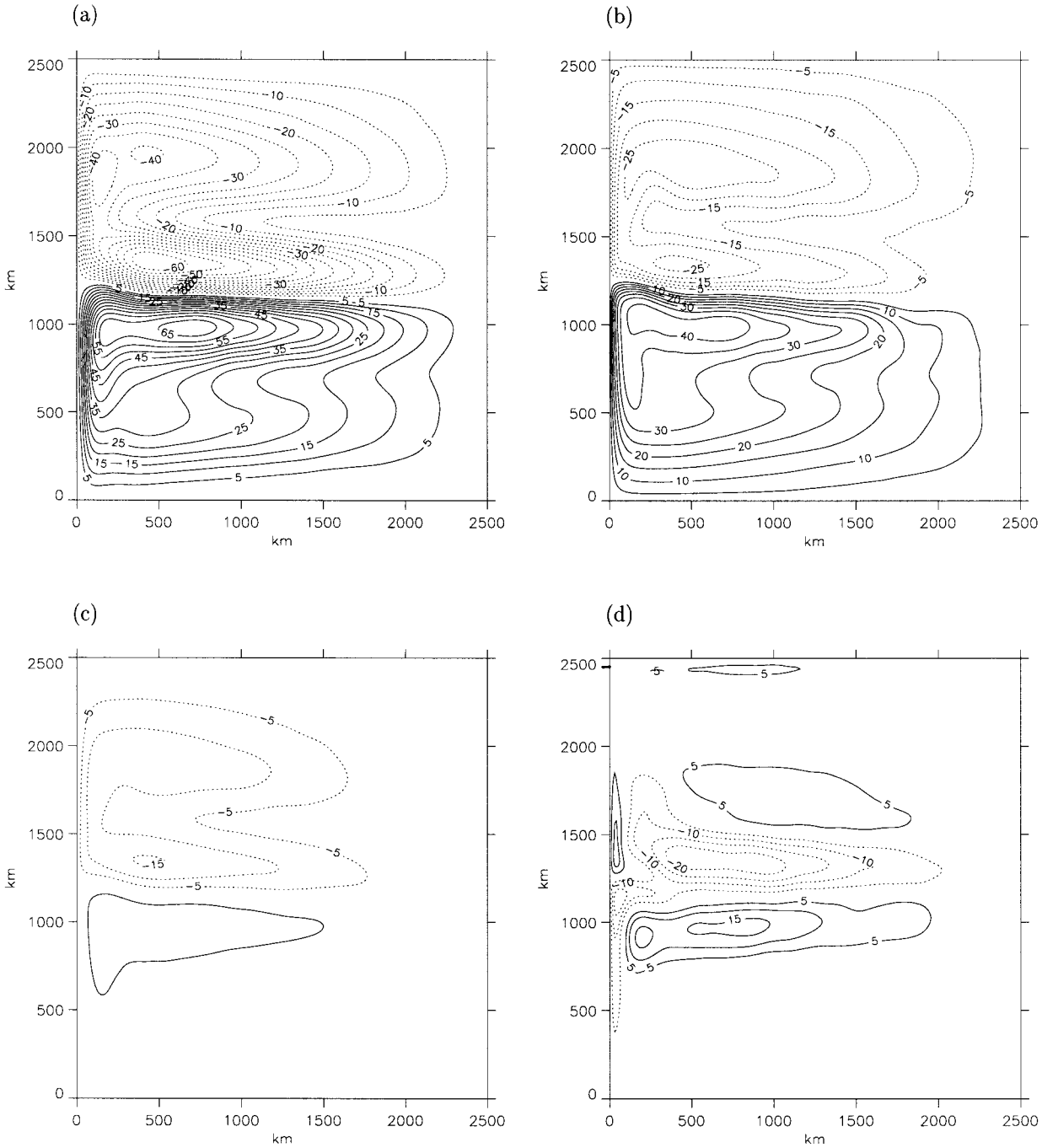

FIG. 1. Streamfunction in Sverdrups (Sv $\equiv 10^6$ m^3 s^{-1}): (a) barotropic streamfunction, (b) streamfunction of layer 1, (c) streamfunction of layer 2, and (d) streamfunction of layer 3.

subpolar gyre shows a marked C-shaped structure in the upper two layers. At the separation point the jet flows southeastward, and associated with this feature the inertial recirculation in the subtropical gyre is stronger than the recirculation in the subpolar gyre. Such an asymmetrical ''jet down'' solution was also found by Jiang et al. (1995) in a reduced-gravity model. It is associated with a pitchfork bifurcation that arises when the ratio of forcing over dissipation parameters (or nonlinearity of the flow) exceeds a critical value. The typical shrinking of the gyres with depth is most clearly visible by comparing the streamfunctions for layers 1 and 3.

In Fig. 2 the average PV for the three layers, together with an instantaneous view of the PV in the upper layer are shown. The PV in the upper layer is dominated by the thickness variations and relative vorticity. In the

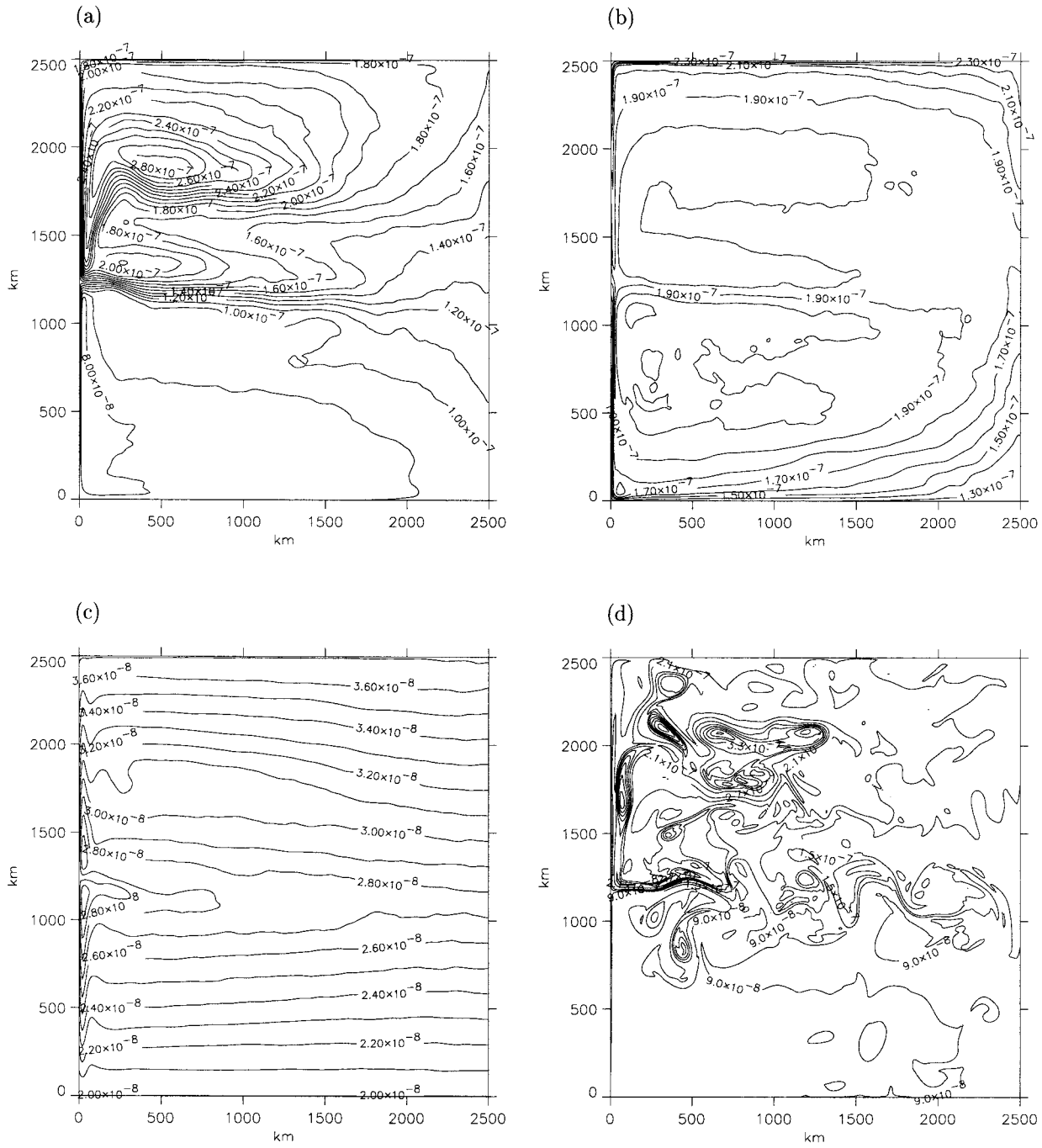

FIG. 2. Potential vorticity (m^{-1} s^{-1}): (a) mean PV of layer 1, (b) mean PV of layer 2, (c) mean PV of layer 3, and (d) instantaneous PV of layer 1.

subtropical gyre PV is relatively well homogenized, divided by a sharp front at the location of the midlatitude jet. The structure of the subpolar gyre reflects a flow regime in which nonlinearities are important. Associated with the C-shaped structure in the flow field is a second strong front where the upper-layer thickness drops to a minimum (see Fig. 3). In the middle layer PV is rather well homogenized within the subpolar and subtropical gyres, with strong fronts near the western, northern, and southern boundaries, and weaker fronts in the midlatitude jet and near the northeastern and southeastern corners of the basin. PV is most homogenized in the middle layer as wind forcing occurs in the upper layer and bottom drag in the bottom layer, in the middle layer

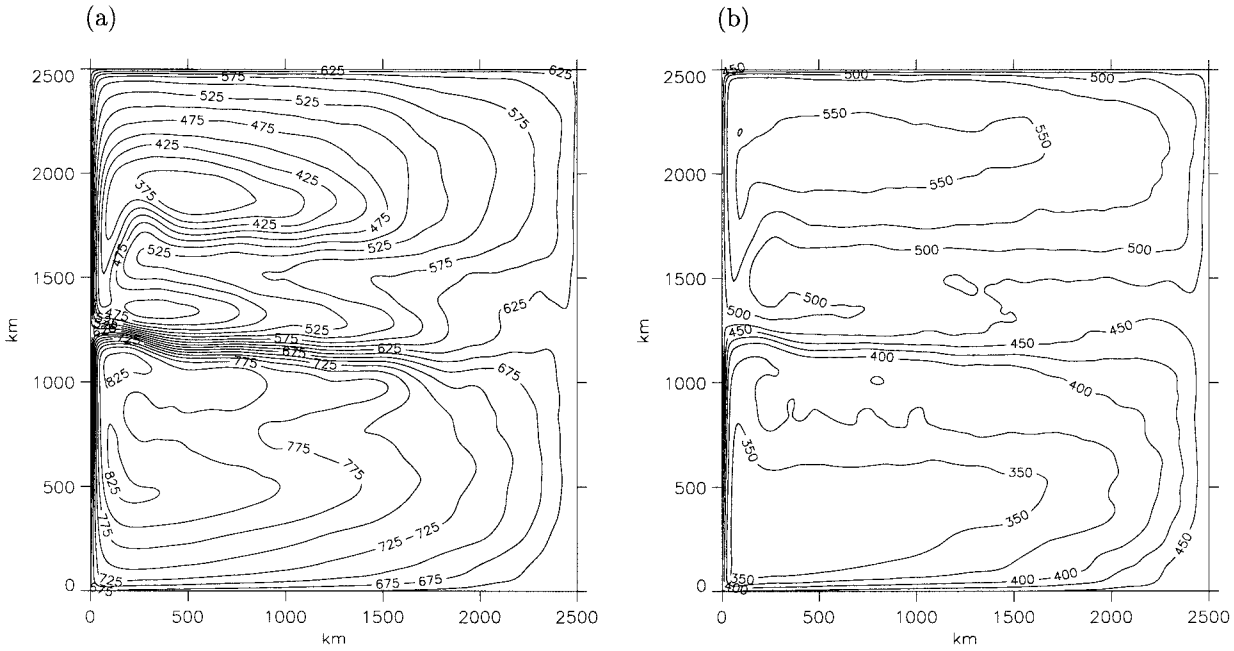

FIG. 3. Layer thickness (m): (a) mean thickness of layer 1 and (b) mean thickness of layer 2.

forcing is absent and dissipation weak. In the lower layer beta (df/dy) dominates. The instantaneous field shows that the flow is unstable. There is abundant eddy activity around the midlatitude jet. The eddies grow on the eastward flowing midlatitude jet and around the C-shaped structure. After pinching off they follow the tight recirculations of both gyres. The mean thickness fields for the upper two layers (Fig. 3) indicate that layer thickness is less well homogenized than PV.

In the midlatitude jet the meridional PV gradient in the second layer is opposite to the PV gradient in the upper layer (Fig. 2). This suggests that baroclinic instability is important. The associated downgradient transport of heat and thickness perturbation is apparent from the overturning streamfunction derived from the meridional eddy transport ($\overline{v'h'}$) (Fig. 4). The clockwise, overturning at the midlatitude jet implies a flattening of the isopycnals by the eddy transports.

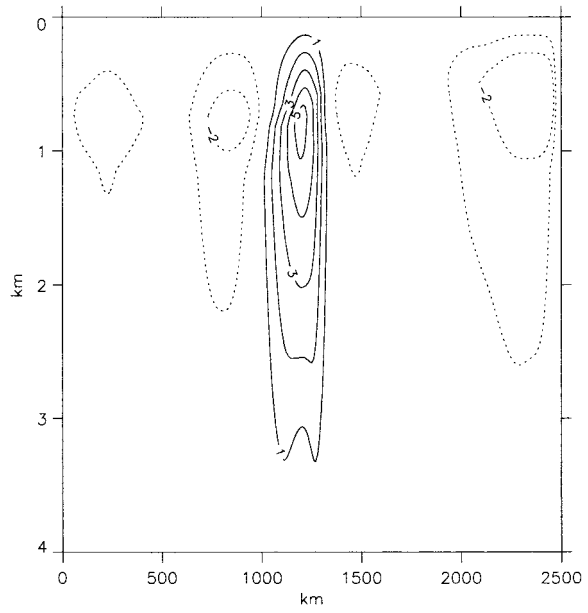

FIG. 4. Eddy-induced overturning streamfunction in Sverdrups: $\phi = \int v_* \, dz$ (the north is to the right and positive numbers indicate clockwise overturning, and $v_* = \overline{v'h'}/\overline{h}$).

4. Local eddy fluxes

a. Divergent and rotational part of fluxes

Usually, when eddy closures are tested in eddy-resolving models, the parameterized fluxes are compared with the diagnosed eddy fluxes. However, as noted by Marshall and Shutts (1981), the diagnosed eddy fluxes have a large rotational component. As the eddy transports arise inside the advection operator [Eqs. (3) and (4)], this part is zero by definition. So locally, one should diagnose only the divergent component of the eddy fluxes when validating eddy closures or diagnosing effective eddy diffusivities. It is only the divergent contribution of the eddy fluxes that must be parameterized.

According to Helmoltz's theorem, any vector field can be separated into its divergent and rotational part, for example, for the eddy thickness flux:

$$\overline{\mathbf{u}'h'} = \overline{\mathbf{u}'h'_R} + \overline{\mathbf{u}'h'_D}, \tag{19}$$

such that

$$\nabla \cdot \overline{\mathbf{u}' h_R'} = 0 \quad \text{and} \quad \nabla \times \overline{\mathbf{u}' h_D'} = 0. \tag{20}$$

The rotational part can be expressed in a streamfunction ψ:

$$\overline{\mathbf{u}' h_R'} = \mathbf{k} \times \nabla \psi. \tag{21}$$

Here, $\overline{u'h'} = -\partial\psi/\partial y$, $\overline{v'h'} = \partial\psi/\partial x$. From Eq. (21) it follows that

$$\mathbf{k} \cdot \nabla \times \overline{\mathbf{u}' h'} = \nabla^2 \psi. \tag{22}$$

For a square basin, the Poisson equation [Eq. (22)] can be solved easily to obtain the (unknown) streamfunction. In fact, in the model code a similar procedure is followed for the barotropic streamfunction. The rotational part of the flow can be deduced from the streamfunction such as defined above, the divergent part follows from Eq. (19). This procedure can be applied to any tracer (e.g., PV). In that case, the function ψ cannot be interpreted as a streamfunction, as it is otherwise dimensioned.

Solving Eq. (22) is only possible if a boundary condition for ψ is supplied. In principal, it is ambiguous what this should be. For the total (divergent plus rotational) mass flux a zero flux condition across the solid boundaries is demanded. The same holds for any other flux. It seems most natural to demand that for the separate divergent and rotational components of the mass flux a zero flux condition also holds. With this boundary condition we have solved Eqs. (22), (21), and (19). This boundary condition is being separately applied to the eddy induced and time-mean flow.

The results of the decomposition for the eddy thickness flux are shown in Fig. 5. Fluxes are evaluated from the 10-yr average. Note that the length of the vectors differ per panel in order to highlight the direction of the flow. The divergent part of the flow appears to be of the same order of magnitude in each layer, while the rotational part is much larger in the directly forced upper layer. In all layers the rotational part dominates the eddy fluxes.

The signatures of meanders and rings are present in the rotational part of the eddy thickness flux (Figs. 5b,d). The effect of individual eddies does not appear in the divergent part of the flow (Figs. 5a,c). However, the impact of the eddy thickness fluxes on the thickness tendency is remarkably clear. In the upper layer the divergent component of the eddy thickness flux is directed toward the north at the midlatitude jet (Fig. 5a). This flow acts to weaken the slope of the isopycnals there. The steep slope implies a large amount of available potential energy, which, in the process of baroclinic instability, is transfered to kinetic energy by weakening the slope of isopycnals. In the lower layer the divergent part of the flow is directed southward, compensating the upper-layer flow. In the middle layer (not shown) the flow is weak. Southward flow at the midlatitude jet dominates, but the velocities are small compared to the upper and lower layer. This circulation induced by the divergent eddy thickness fluxes is in agreement with the eddy-induced overturning in Fig. 4.

Figure 6 shows that the eddy PV flux generally flows in the opposite direction of the eddy thickness flux (Fig. 5), in agreement with the fact that the mean fields of PV and thickness have opposite gradients (Figs. 3 and 2). It is also clear from Figs. 6a,c that the divergent eddy PV flux tends to be of smaller scale than the divergent eddy thickness flux. The eddy PV flux is dominated by large values in the region of confluence of the western boundary currents and separation of the midlatitude jet. In the second layer the eddy PV fluxes are small. In Fig. 7 the upper-layer eddy PV flux is decomposed into contributions from a relative vorticity term and a stretching term; resulting from the decomposition $q = \zeta/h + f/h$. This figure demonstrates that the large eddy PV fluxes near the jet separation result from the relative vorticity contribution. Where the flow is strong (midlatitude jet, western boundary currents, and C-shaped structure), the relative vorticity term and stretching term are of equal importance in the eddy fluxes. The important role of the relative vorticity is associated with the scale of the eddies. The large-scale PV field is dominated by the stretching term; it is controlled by thickness variations and toward the eastern boundary by the planetary vorticity gradient.

The ratio of ζ and f is the Rossby number, which is everywhere small, apart from the western boundary currents and the western part of the midlatitude jet. But also there it is smaller than one. The same holds for the total flux of PV and the flux of PV by the mean flow (not shown), but now the relevant nondimensional number is a gradient Rossby number, namely the minimum of $\nabla\zeta/\beta$ and $h\nabla\zeta/f\nabla h$. In general the latter term is the smallest. Here $h\nabla\zeta/f\nabla h$ can be written as $\zeta/f \times L_h/L_\zeta$, where L_h and L_ζ are the lengthscales of h and ζ, respectively. For the gyre-scale flow where the Rossby number is low, L_h/L_ζ is larger than one and the relevant gradient Rossby number for the fluxes is larger than the Rossby number for the mean flow. For the midlatitude jet where the Rossby number is larger, however, L_h and L_ζ are both determined by the jet width and their ratio is one. So, both for the mean flow and mean fluxes the (gradient) Rossby number is maximized by $U/(fL)_{\text{jet}}$. The ratio of the eddy fluxes of ζ/h and f/h is again $h\nabla\zeta/f\nabla h$. Now, the ∇ terms denote eddy quantities while the h in the numerator is assigned to a mean flow quantity. The relevant gradient Rossby number for the eddy fluxes becomes $U/(fL)_{\text{eddy}} \times h_{\text{jet}}/h_{\text{eddy}}$, which is much larger than the mean flow Rossby number suggests. As a result, the eddy fluxes possess a much larger Rossby number than the mean flow fluxes.

b. Eddy fluxes and mean gradients

The divergent eddy fluxes can be decomposed into cross- and along-gradient contributions. Figure 8 shows that in the upper layer the downgradient eddy fluxes (pos-

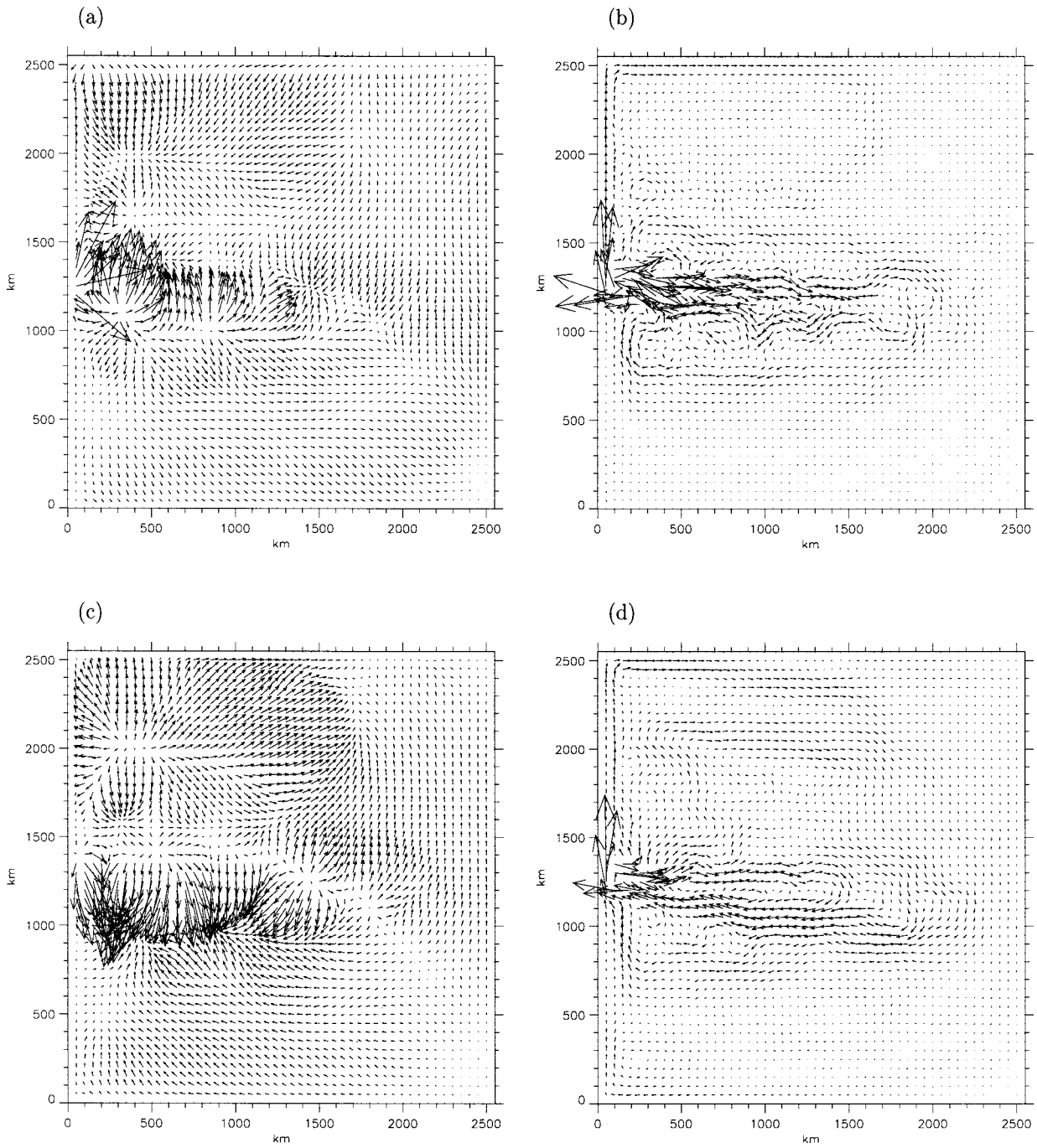

FIG. 5. Divergent and rotational part of the eddy thickness flux. Maxima are stated between brackets. Largest vector in the plot corresponds to the maximum; vectors are plotted every fifth grid point. (a) Divergent layer 1 (4.9 $m^2\ s^{-1}$), (b) rotational layer 1 (41.4 $m^2\ s^{-1}$), (c) divergent layer 3 (2.4 $m^2\ s^{-1}$), and (d) rotational layer 3 (8.5 $m^2\ s^{-1}$).

itive values) dominate the upgradient transfer for both PV, f/h, and layer thickness. Only the fluxes in the central, western part of the basin are shown. Outside this area the fluxes are small. Again, we note that the downgradient flux of PV is more confined to the jet separation, due to the relative vorticity contribution. The downgradient fluxes of both f/h and thickness extend farther eastward in the midlatitude jet. It is also clear from Fig. 8 that along-gradient components for both PV and f/h are more important than in the case of the thickness fluxes. This would suggest that the effect of eddy fluxes on the mean flow tends to be more local in case of layer thickness than in case of PV. This would be an argument in favor of a local diffusive closure for layer thickness.

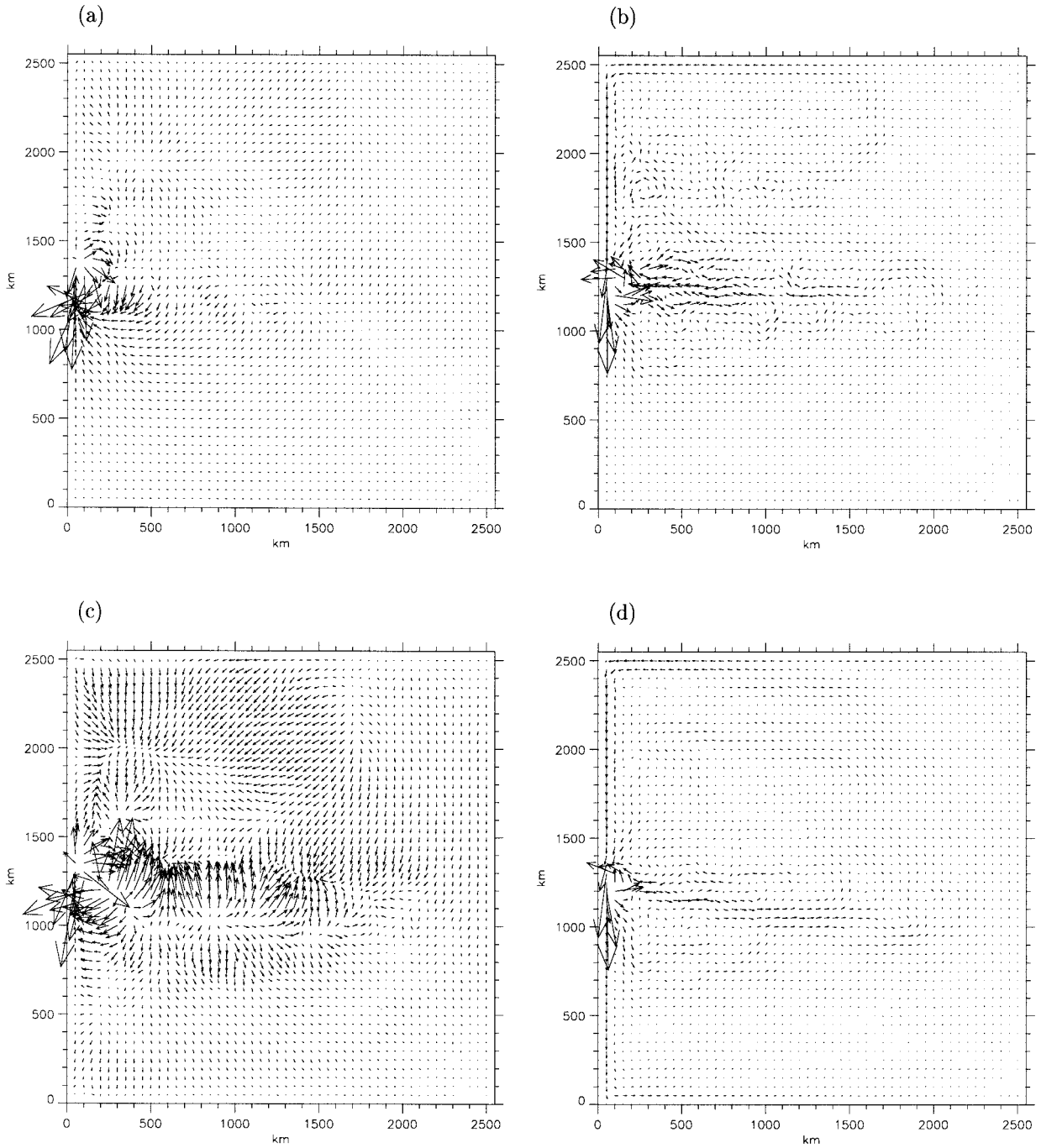

FIG. 6. Divergent and rotational part of the eddy PV flux; vectors are plotted every fifth grid point. (a) Divergent layer 1 (7.6×10^{-9} s^{-2}), (b) rotational layer 1 (25.6×10^{-9} s^{-2}), (c) divergent layer 3 (0.4×10^{-10} s^{-2}), and (d) rotational layer 3 (0.3×10^{-9} s^{-2}).

There are a number of possible explanations for an increased importance of along-gradient fluxes in case of PV. Following Rhines and Holland (1979) we write the eddy flux of q by integrating the (eddy) vorticity equation, following the fluid, and multiplying all terms with the eddy velocity u' and taking a time average. This becomes

$$\overline{u_i' q'} = -\kappa_{ij} \frac{\partial \overline{q}}{\partial x_j} + \overline{u_i' \int_0^t (F_q - D_q)\, dt'} + O(\gamma_q), \quad (23)$$

where $\kappa_{ij} = \overline{u_i'(\mathbf{x}, t)[x_j(t) - x_j(0)]} = \overline{u_i' x_j'}$; $\mathbf{x}(t)$ or $x_j(t)$, is the Lagrangian position of a fluid particle at time t and x_j' is the particle displacement.

One possible cause for large along-gradient fluxes is

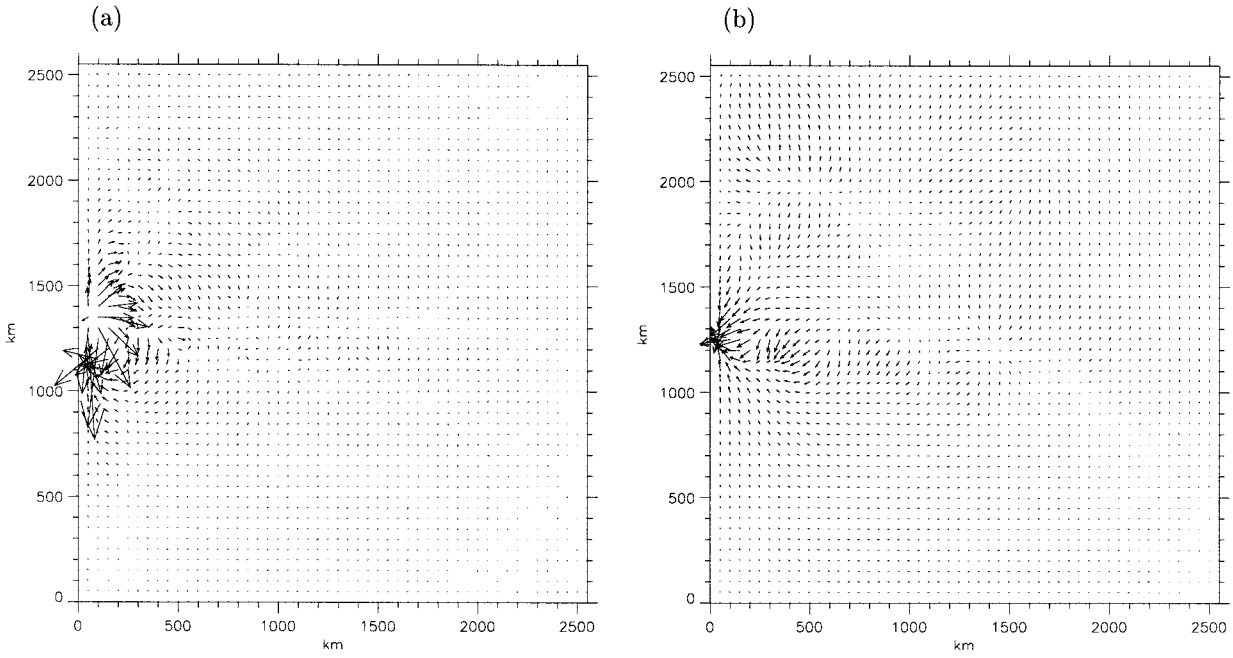

FIG. 7. Divergent part of the separate terms in the eddy PV flux for layer 1, scaled with the largest vector of the the divergent eddy PV flux (7.6×10^{-9} s^{-2}): (a) ζ/h and (b) f/h.

a skew κ_{ij}; for instance, when $\overline{u'q'} = -\kappa_{12}\partial\overline{q}/\partial y$ (neglecting the forcing and dissipation). From Eq. (23) we see that this arises when $\overline{u'y'}$ and $\overline{v'x'}$ are large. Note, that u' and v' here only describe the divergent flow. Also, $\overline{u_i' \int_0^t (F_q - D_q)\, dt'}$ can give rise to departures from a local diffusive closure. In the discussion we will address this further.

The eddy diffusivity for PV and layer thickness is shown in Fig. 9. Locally, very high point values can occur with diffusivities larger than 10 000 m^2 s^{-1}. To display the overall pattern of the diffusivity we used cutoff values of plus and minus 500 m^2 s^{-1}. Also, we smoothed all values with a boxcar average with a width of five grid points. On the average the values for the eddy diffusivity are smaller than calculated in Holland and Rhines (1980), as we consider only the divergent fluxes. The eddy diffusivity for layer thickness shows roughly the same structure for each layer. In the eastern part of the midlatitude jet the diffusivity of thickness is negative, also to the north and south of the jet and in the central parts of the wind-driven gyres the diffusivity is negative. These are the main areas of eddy decay. In general, regions of positive eddy diffusivity dominate. Moreover, in regions of negative eddy diffusivity the mean flow and eddy fluxes are weak. Most important regions of positive eddy diffusivity are the midlatitude jet in the western three-quarters of the domain and the northern and southern part of the basin where the slow westward recirculation of the wind-driven gyres takes place. Regions with a positive eddy diffusivity are associated with eddy production. In most cases, eddy production is accomplished by baroclinic instability. The conversion from mean to eddy potential energy is accomplished by a thickness transport down the mean thickness gradient. In regions where eddy activity is dying away, upgradient eddy fluxes are to be expected (Rhines 1977). The eddy potential energy is converted back to mean potential energy and the eddy thickness flux is up the mean gradient.

In the upper layer, the pattern of the eddy diffusivity for PV is very similar to that for thickness, but the overall structure is somewhat noisier, and the regions with a negative diffusivity are larger. In the second layer where PV homogenization is most outstanding, the pattern of diffusivity is dominated by smaller scale features. The overall pattern of diffusivity in the third layer deviates most from that in the first layer, with very weak diffusivities in the eastern part and very low diffusivities in the northern and southern part of the basin. The pattern of diffusivity and the enhanced variance on smaller scales is also visible in the diffusivity of the f/h part of the PV (not shown). The diffusivity patterns for f/h and PV are rather similar, apart from the western boundary currents. Here, the diffusivity of PV is more determined by the diffusivity of ζ/h. This suggests that, where the gradients are weak and the relevant quantity is well-mixed, or homogenized, the eddy diffusivity is less well determined and becomes noisier. As PV is better homogenized than layer thickness the eddy diffusivity for PV is noisier. In itself, this does not imply that the PV closure is wrong. The same problem would occur for layer thickness if the layer thickness was forced to be nearly uniform. In the real ocean, however, there is more support for the occurrence of large regions of nearly uniform PV than of nearly uniform layer thickness (McDowell et al. 1982).

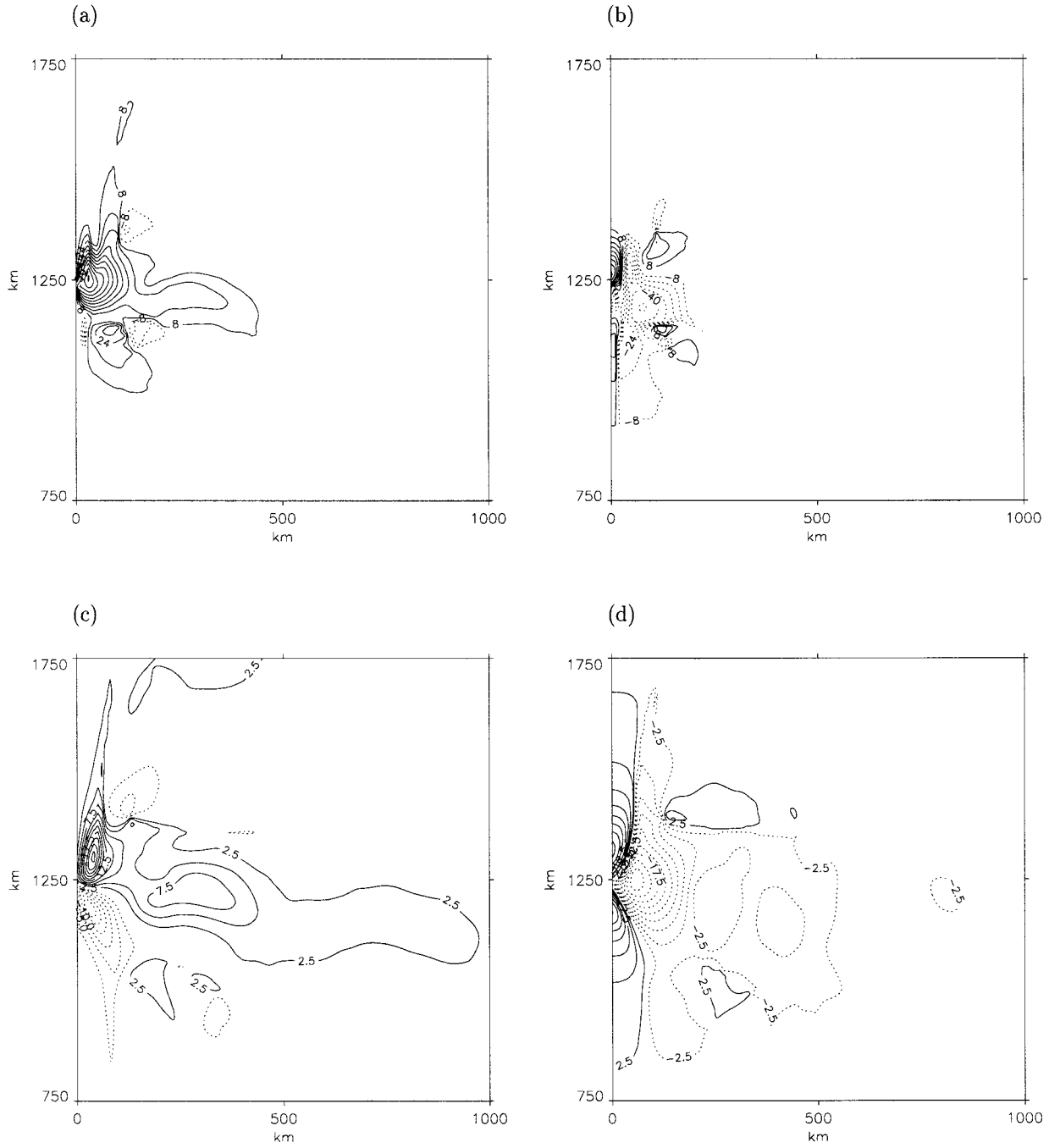

FIG. 8. Down- and along-gradient components of the eddy fluxes in the upper layer for the central western part of the basin: $x = 0$–1000 km; $y = 750$–1750 km. (a) Downgradient eddy flux of PV in 10^{-10} s^{-2}, (b) along-gradient eddy flux of PV, (c) downgradient eddy flux of

5. Zonally averaged flux–gradient relations

a. Zonally averaged profiles

The zonally averaged (divergent) eddy thickness transport is presented in Fig. 10, together with the zonally averaged meridional thickness gradient. As near the boundaries the flux–gradient relation may be affected by the boundary effects we have left out the upper and lower 250 km of the (2500 km) basin. Figure 10 reveals the picture that already emerged from section 4. In the upper layer, the meridional eddy thickness flux is positive at the midlatitude jet (Fig. 10a). The positive eddy transport can be understood from the meandering of the jet. A northward displacement of the jet will result in anomalous northward transport of relatively thick water columns: $v'h' > 0$. A southward displacement results

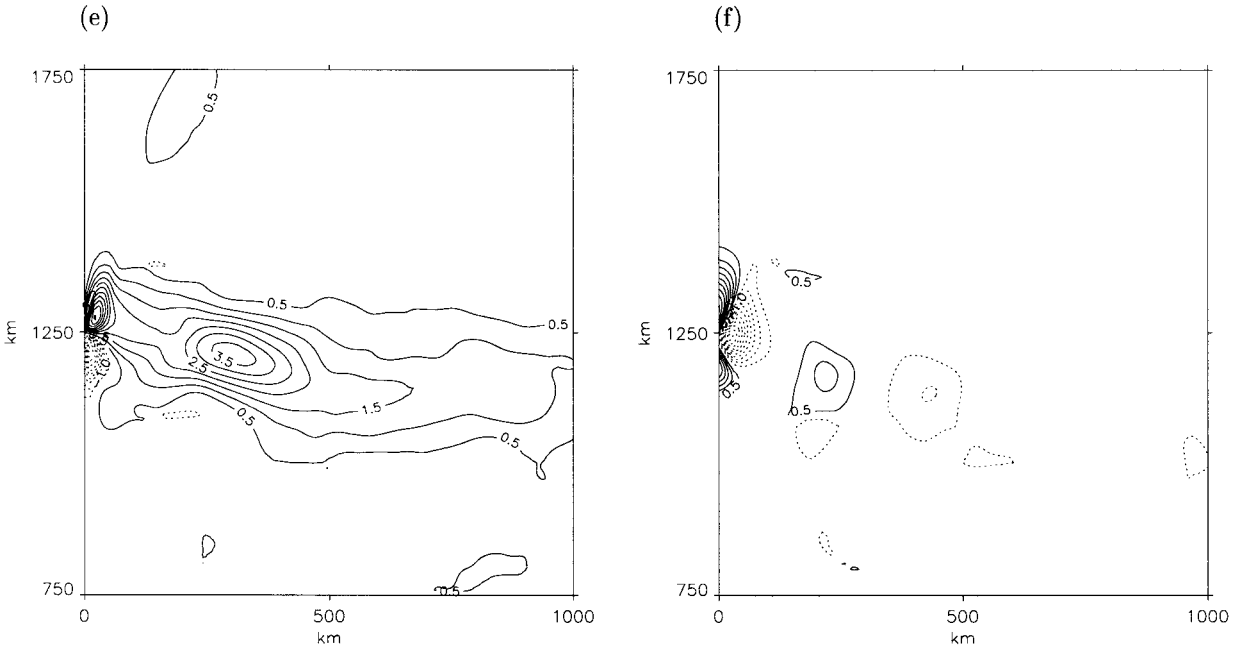

FIG. 8. (*Continued*) f/h, (d) along-gradient eddy flux of f/h, (e) downgradient eddy flux of thickness in $m^2\ s^{-1}$, and (f) along-gradient eddy flux of thickness. Figures are contoured with about 10% of the maximum absolute value.

in an anomalous southward transport of anomalous thin layers, so also $v'h' > 0$. The eddy flux in the upper layer is mainly compensated in the lower layer. The middle layer is relatively inactive. Zonally averaged, the eddy flux in the second layer also compensates partly the eddy flux in the upper layer. In general, the zonally averaged mean meridional gradients roughly has the same shape as the zonally averaged (divergent) eddy fluxes.

Similar features are visible in the eddy flux of PV (Fig. 11), but the transport and gradient are in the opposite direction, which is expected given how PV and thickness fluxes relate on the large scale. In the upper layer, the slope in PV across the northern jet associated with the C-shaped inertial recirculation in the subpolar gyre is much stronger compared to the slope in thickness, as especially the inverse of the layer depth becomes large there (cf. Figs. 10a, 11a and Figs. 2a, 3a). It is apparent from Fig. 11a that the eddy flux of PV does not scale with the meridional PV gradient in the subpolar gyre, especially at the internal front associated with the C-shaped structure of the inertial recirculations. Also, the peaks in PV gradient and eddy flux of PV are displaced with respect to each other, most noticeably in the upper layer. This is primarily caused by the eddy transport of ζ/h. This eddy flux does not scale very well with either the meridional gradient in PV or in ζ/h itself.

Almost everywhere the zonally averaged eddy fluxes are down the mean gradient. Despite the good correspondence of the shape of the curves of zonally averaged eddy fluxes and mean gradients, the amplitude of the inversely derived eddy diffusivity, that is, the ratio of eddy flux and mean meridional gradient, varies greatly. It is clear that κ is much larger at the latitude of the midlatitude jet than away from the jet. A second maximum in the eddy diffusivity exists near the return flow of the C-shaped inertial recirculation in the subpolar gyre, but only for layer thickness.

b. Least squares fits

The effective eddy diffusivity can be determined by a linear (least squares) fit between the eddy fluxes and the mean meridional gradient. We do not show pointwise scatterplots as these are too noisy. Instead, scatterplots of the zonally averaged data are shown (see Fig. 12). When calculating eddy diffusivities and correlation coefficients we omit low values in either flux or gradient, that is, when the absolute values are less than one per mill of the maximum. We do so, in order that the calculations are not flawed by excessive noise associated with extremely low values in either component. In the upper layer we find an effective eddy diffusivity of 550 $m^2\ s^{-1}$, with a correlation coefficient of 0.92. For the second layer we get $\kappa_h = 280\ m^2\ s^{-1}$. However, the correlation coefficient is smaller (0.72). For the third layer the largest value of κ_h is found: 700 $m^2\ s^{-1}$ (correlation 0.92). All correlations mentioned here and in the following are significant at the 99.9% level according to a Student's t-test. For all three layers the best fit is obtained in the midlatitude jet (diamonds) where the fluxes and gradients are large. Within the gyres the flux–

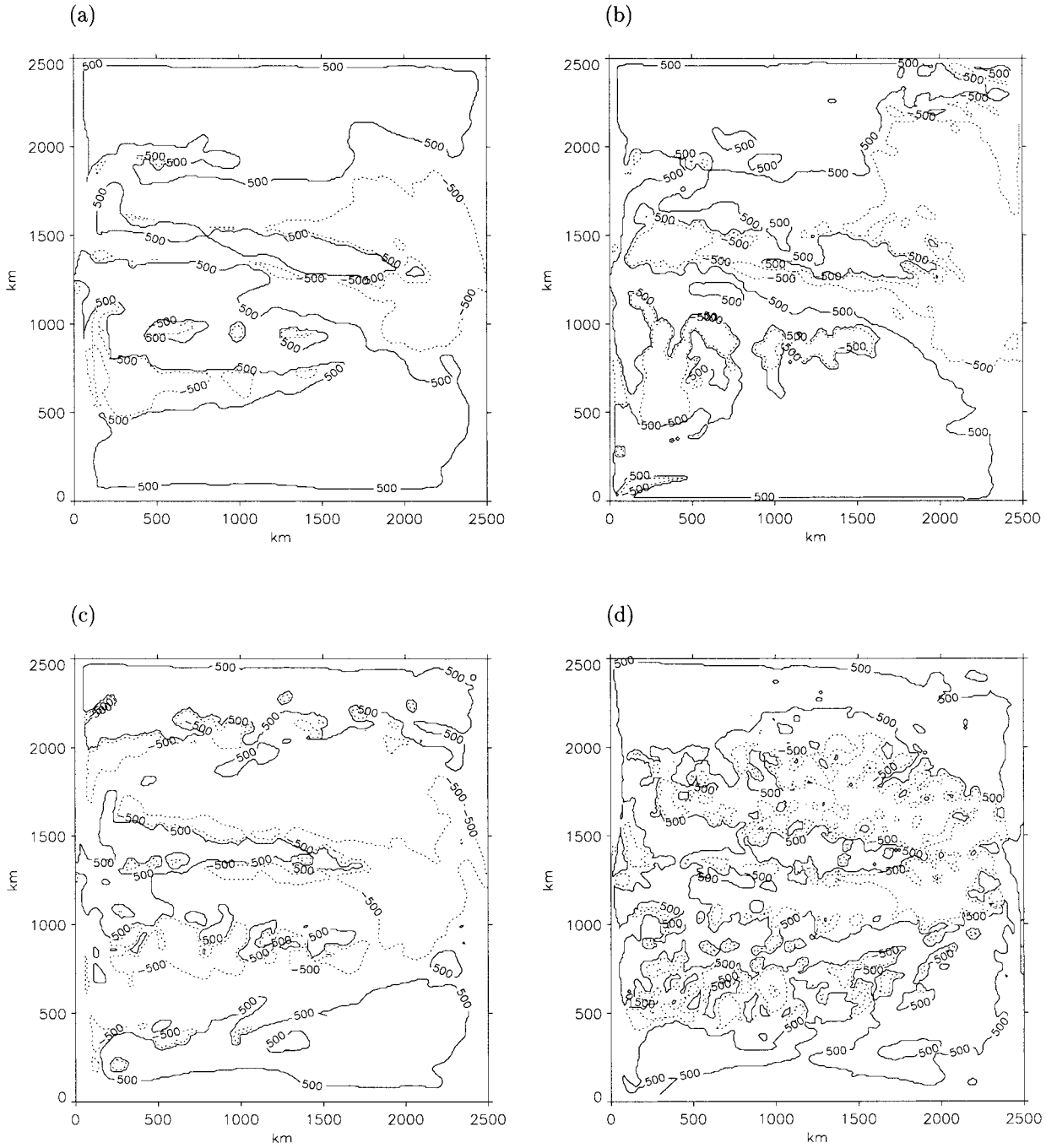

FIG. 9. The effective eddy diffusivity (in $m^2\ s^{-1}$); a cutoff value of 500 $m^2\ s^{-1}$ has been used. (a) For thickness in layer 1, (b) for PV in layer 1, (c) for thickness in layer 2, (d) for PV in layer 2, (e) for thickness in layer 3, and (f) for PV in layer 3.

gradient relation shows multifunctional behavior, the gradients, however, are very small. Rix and Willebrand (1996) evaluated eddy diffusivities from the WOCE–CME model and found $\kappa_h = 1000\ m^2\ s^{-1}$. They investigated a limited domain of the North Atlantic, south of 30°N. Analyses of both observations and more comprehensive ocean models suggest that the eddy diffusivity is related to the mean flow and varies with the eddy energy (Stammer 1998; Bryan et al. 1999).

The larger diffusivity in the lower layer and weaker diffusivity in the middle layer is associated with the fact that the return flow of the eddy-induced meridional overturning occurs on deeper levels than the decrease of the isopycnal slope with depth suggests. Apparently, in the

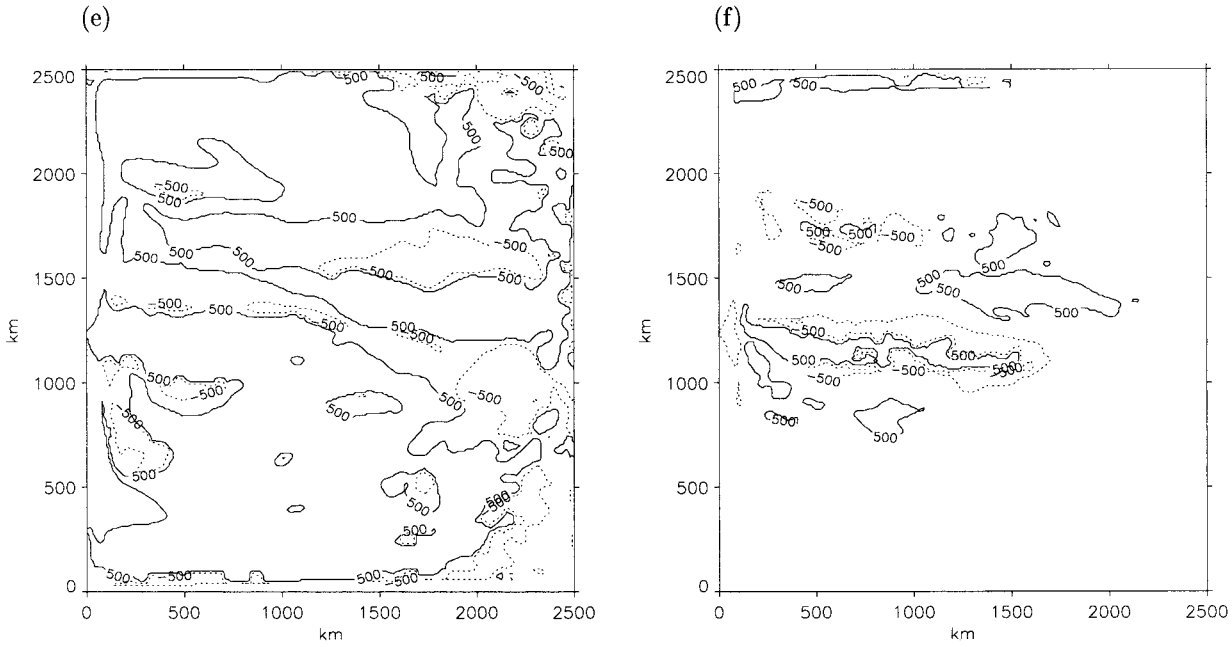

FIG. 9. (*Continued*)

vertical the eddy fluxes are partly determined by integral constraints and not only by local gradients. Moreover, the vertical structure of the eddies is determined by the vertical profiles of density and Brunt–Väisälä frequency. Also, they tend to become more barotropic between the phase of linear growth and nonlinear equilibration in accordance with the theory of geostrophic turbulence (Rhines 1977). Killworth (1997) and Treguier et al. (1997) stressed the vertical dependence of the eddy diffusivity. Our results do not confirm, however, the vertical profiles found in the channel models of Killworth (1998) and Treguier (1999), that is, maximal diffusivity at middepth. This may be associated with the different geometry (channel vs closed basin) and flow regime, our study being the more nonlinear. It also could be that the low vertical resolution used in the present model is not able to resolve the vertical profile of the eddy diffusivity adequately. A minimum value at middepth, however, as found here, is absent in their calculations.

Also, the eddy flux of PV is better represented by the gradient of the mean PV in the upper and lower layer than in the middle layer (see Fig. 13). For the upper layer we obtain a value of 630 $m^2\ s^{-1}$ (correlation coefficient of 0.71). Figure 13a shows two lines of points. In the anticyclonic gyre the gradients are very small and nearly all points (asterisks) cluster around the (0,0) point. The cyclonic gyre is divided in a northern and southern part by a strong PV front; see Fig. 2a. In the southern part the fluxes are weak. The points (plus signs) form a nearly horizontal line in Fig. 13a. In the northern part the diffusivity is larger and the points fall along the average regression line. The midlatitude jet (diamonds) shows a distinct multifunctional flux–gradient relation. The stronger diffusivities are found at the northern flank, the weaker at the southern flank. For the middle layer we obtain κ_q is 290 $m^2\ s^{-1}$ (correlation 0.58). Here the eddy fluxes vary considerably while the mean gradient remains weak. In the lower layer we get a κ_h of 690 $m^2\ s^{-1}$ (correlation 0.80).

The significance for the differences in correlation for the thickness closure versus the PV closure using Fisher's z transformation (Press et al. 1986) is larger than 0.999 for the upper layer, 0.988 for the middle layer, and larger than 0.999 for the third layer. So, although the values of κ_q and κ_h are roughly the same, as well as their variation with depth, the fit for κ_q is not so good as it is for κ_h. The eddy fluxes of ζ/h show a much weaker correlation with the mean PV gradient, which negatively biases the correlation for κ_q, for instance, 0.47 in the upper layer. On the other hand, the correlation for the eddy diffusivity of f/h only marginally improves on that of κ_q; 0.75 versus 0.71 in the upper layer, respectively, and it is still much weaker than the correlation for κ_h (0.90).

In principle, a weaker correlation in estimating a linear fit between eddy fluxes and mean-flow gradients does not disclaim the possibility of a good closure relation between the two. It only disclaims that this can be done with a constant diffusivity factor. Figure 13a, for instance, clearly shows the existence of different regimes with a different κ_q. Now, if the scatterplot would have shown a strongly curved line, this would have suggested that a local closure exists, but with a flow-dependent κ_q. Figure 13a shows more a bilinear, or even elliptic curve. This means that a given meridional gradient in the PV field can give rise to two completely different eddy fluxes,

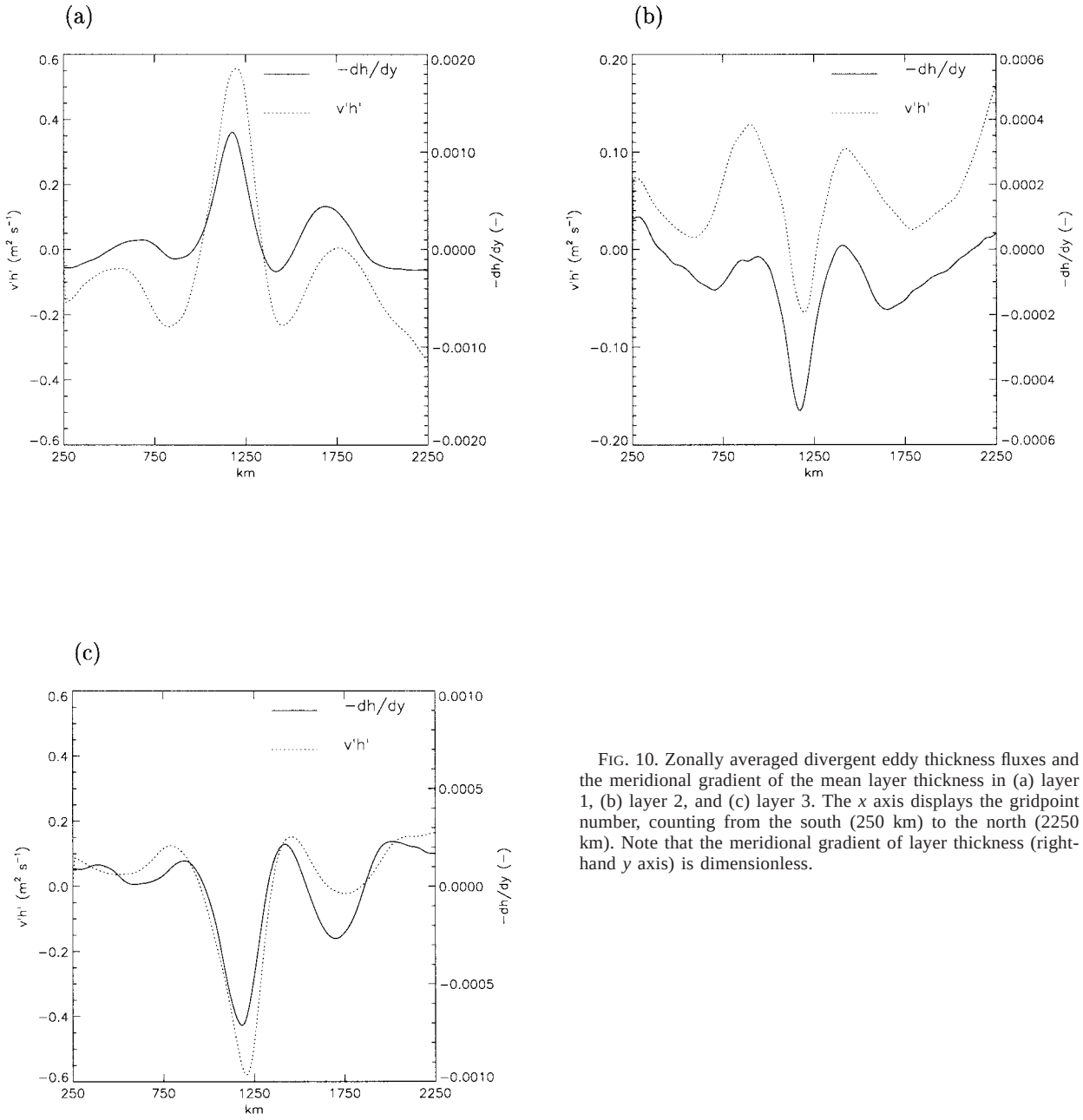

FIG. 10. Zonally averaged divergent eddy thickness fluxes and the meridional gradient of the mean layer thickness in (a) layer 1, (b) layer 2, and (c) layer 3. The *x* axis displays the gridpoint number, counting from the south (250 km) to the north (2250 km). Note that the meridional gradient of layer thickness (right-hand *y* axis) is dimensionless.

depending on either a nonlocal feature, or, another flow characteristic that has not been accounted for. This suggests the possibility that within a more limited domain with more homogeneous flow characteristics or a weaker relative vorticity, a better linear fit between eddy fluxes of PV and mean PV gradients can be found.

We have intensively searched for regions in which the fit between between PV fluxes and PV gradients was as good, or even better than the fit between thickness fluxes and gradients. It appears that such regions exist, but only if the mean PV gradient is either not too weak or not too strong. If it is too weak, for instance, in the third layer where β dominates the PV gradient, or within the homogenized pools in the middle layer, the flux gradient–relation for PV becomes too noisy and a flux–gradient relation for thickness is better defined. If the PV gradient becomes too strong, for instance in the midlatitude jet and most parts of the subpolar gyre in the two upper layers, the role of relative vorticity becomes too important in the eddy PV fluxes, and the flux–gradient relation gets flawed. In between is a regime where the eddy PV fluxes still can be approximated by the flux of f/h, but gradients in h are so strong that they dominate the mean PV gradient: $10^{-14}\ \mathrm{m^{-2}\ s^{-1}} < |\partial q/\partial y| < 10^{-13}\ \mathrm{m^{-2}\ s^{-1}}$.

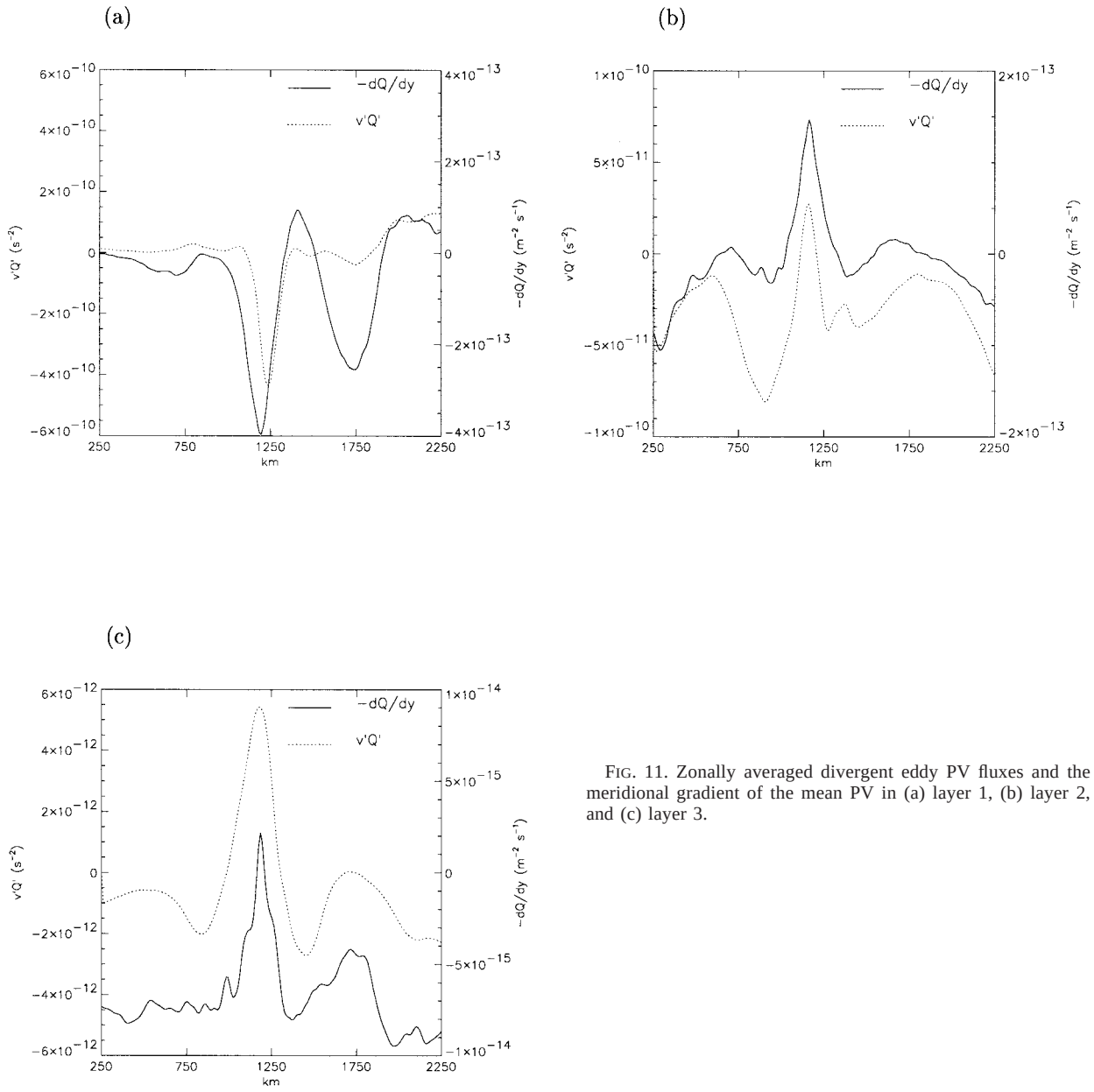

FIG. 11. Zonally averaged divergent eddy PV fluxes and the meridional gradient of the mean PV in (a) layer 1, (b) layer 2, and (c) layer 3.

This condition is fulfilled in the northern half of the cyclonic gyre. In the upper layer, PV gradients are weak in the subtropical gyre and the southern half of the cyclonic gyre, but well away from the midlatitude jet (Fig. 2a). In the northern half of the cyclonic (subpolar) gyre a definite flux–gradient relation exists while the gradients are either not too weak and not too strong. In the middle layer, gradients become moderately weak where the homogenized pool is bounded by a region where the upward doming of isopycnals is weakening toward the northern boundary (Figs. 2b and 3). Figure 14 displays scatterplots for the eddy diffusivity in PV and thickness for these regions. Here, κ_q for layer 1 and 2 are 474 m^2 s^{-1} and 840 m^2 s^{-1}, with correlation coefficients of 0.94 and 0.97, respectively; κ_h for layers 1 and 2 are 527 m^2 s^{-1} and 700 m^2 s^{-1}, with correlation coefficients of 0.88 and 0.90. The significance for the differences in correlation is 0.929 for the upper layer and 0.999 for the second layer. Note that in this flow regime a maximum diffusivity at middepth occurs, in accordance with the results of Killworth (1998) and Treguier (1999).

6. Discussion

Since the introduction of a parameterization by Gent and McWilliams (1990) for the eddy-induced velocity

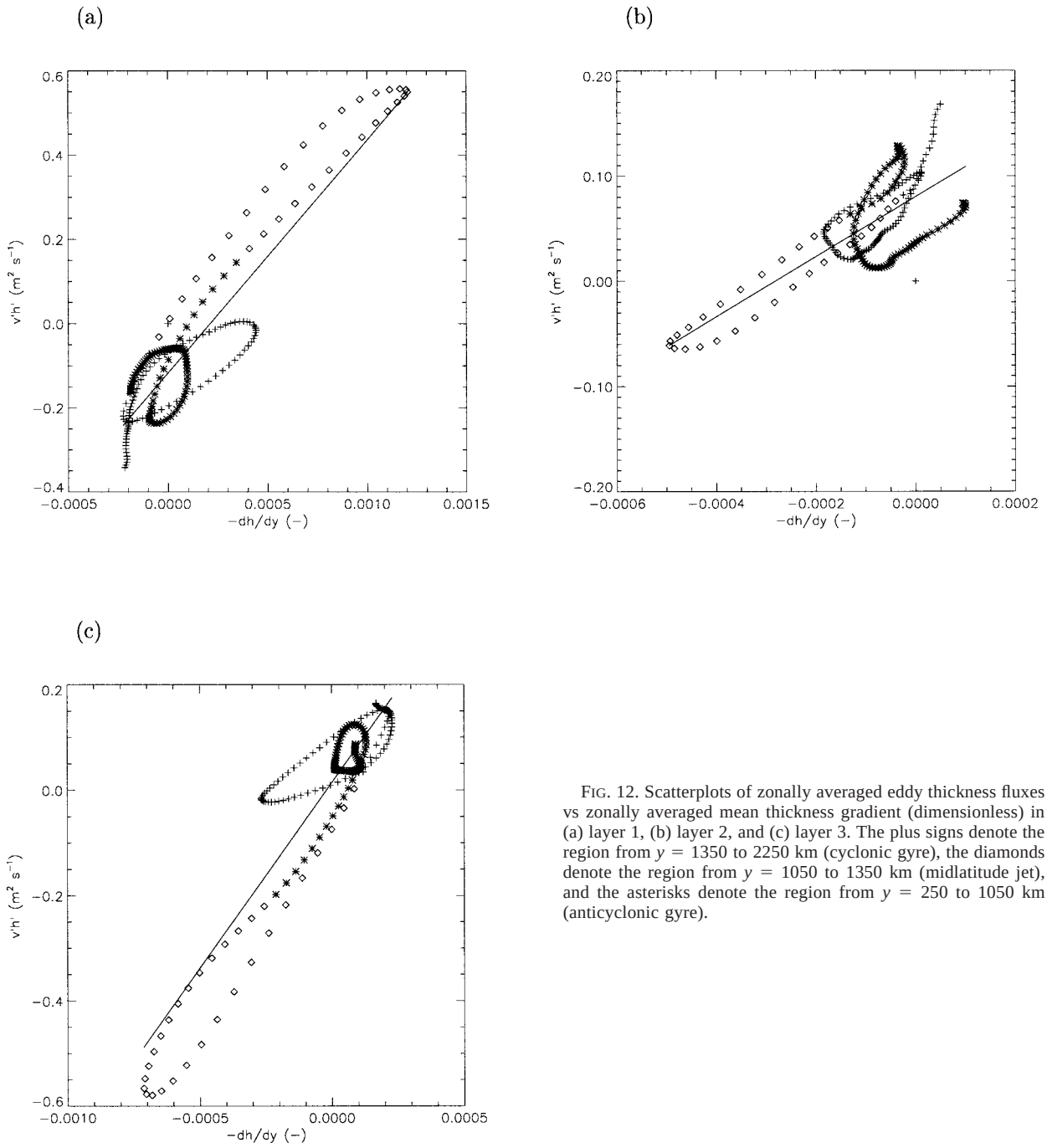

FIG. 12. Scatterplots of zonally averaged eddy thickness fluxes vs zonally averaged mean thickness gradient (dimensionless) in (a) layer 1, (b) layer 2, and (c) layer 3. The plus signs denote the region from $y = 1350$ to 2250 km (cyclonic gyre), the diamonds denote the region from $y = 1050$ to 1350 km (midlatitude jet), and the asterisks denote the region from $y = 250$ to 1050 km (anticyclonic gyre).

that advects tracers in addition to the Eulerian mean flow, there is an ongoing debate on whether this parameterization should be equivalent to downgradient diffusion of thickness or downgradient diffusion of PV. In some reentrant channel models it was found that downgradient diffusion of PV is a better description of the effect of eddies on the mean flow than a downgradient diffusion of thickness (Lee et al. 1997; Killworth 1998; Treguier 1999; Marshall et al. 1999). In the present closed basin study we do not confirm this result. In the contrary, a downgradient diffusion of thickness appears to be a better description of the divergent eddy fluxes than a downgradient diffusion of PV. It is not completely clear what causes this difference. It has been observed that within closed basins another PV and enstrophy balance occurs than within channel models (Holland and Rhines 1980). The mean PV field is more curved and zonally asymmetric, with eddy generation in the west

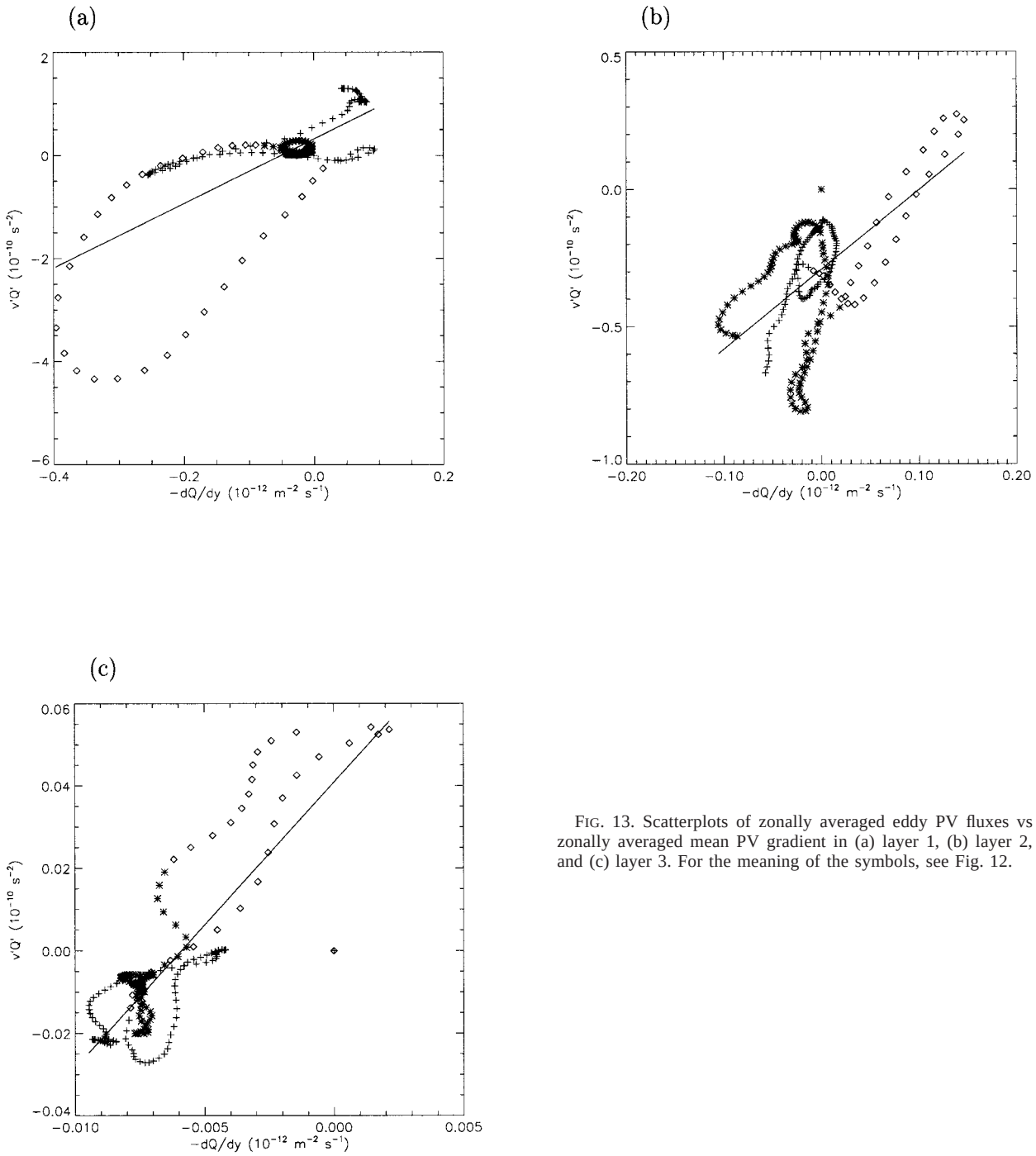

FIG. 13. Scatterplots of zonally averaged eddy PV fluxes vs zonally averaged mean PV gradient in (a) layer 1, (b) layer 2, and (c) layer 3. For the meaning of the symbols, see Fig. 12.

and eddy decay in the east of the midlatitude jet, and with additional eddy generation areas in the westward return flows. Also, the balance between cross-gradient eddy transport of PV and dissipation [Eq. (13)] is less exact within closed basins.

A further difference is that we consider a more nonlinear flow regime in which ageostrophic effects are more important. This may explain at least some of the discrepancies between our findings and previous results, as for moderate PV gradients a closure for PV works as well or even better than a closure for layer thickness. For stronger gradients this is not the case due to the increasing role of the relative vorticity contribution to the eddy PV flux. The flux of relative vorticity (divided by layer thickness) does not scale with the mean PV gradient. On the other hand, also for weak gradients a

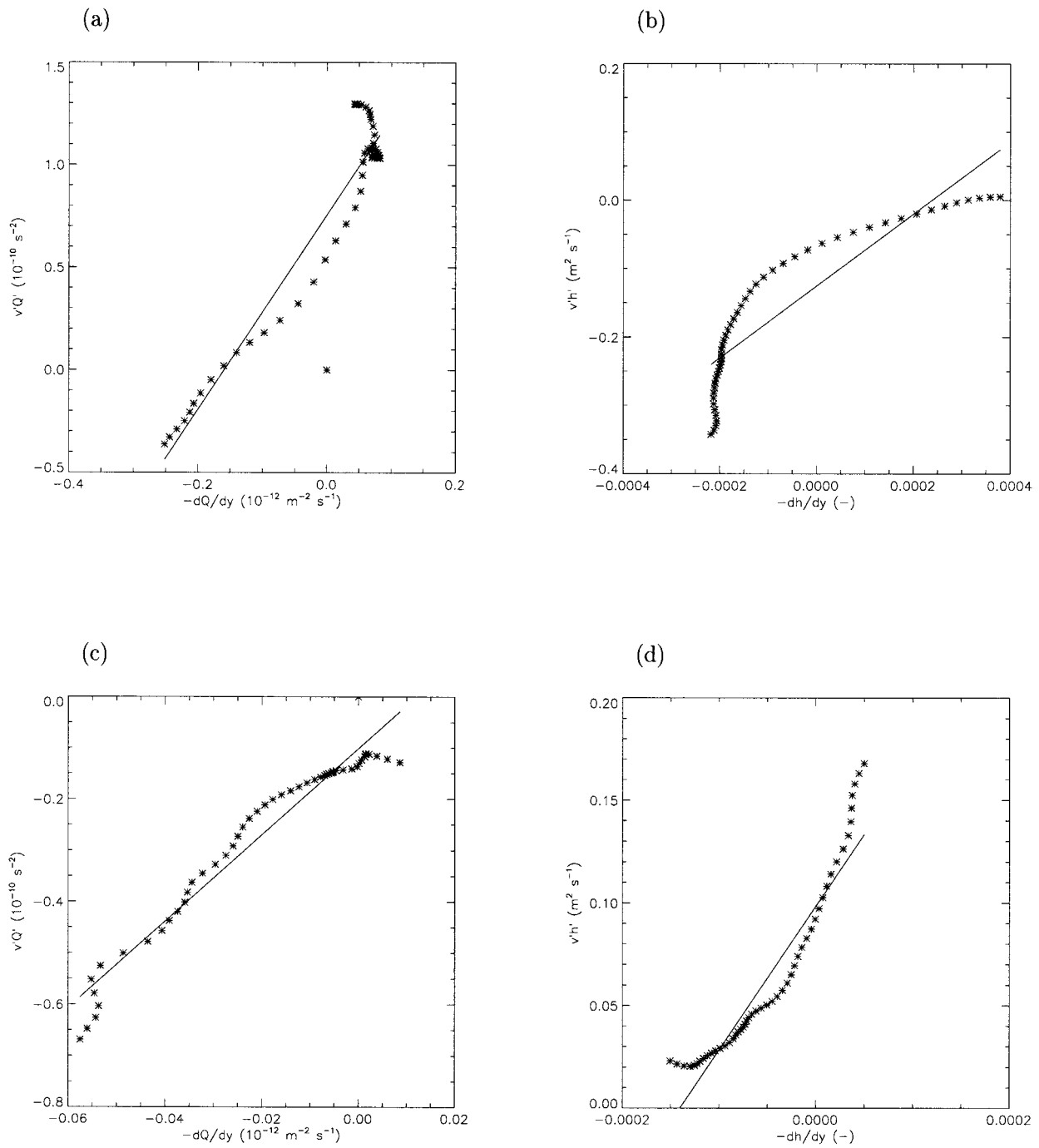

FIG. 14. Scatterplots of zonally averaged eddy fluxes vs zonally averaged mean gradients between 250 and 750 km from the southern boundary. (a) Potential vorticity in the upper layer, (b) thickness in the upper layer, (c) PV in layer 2, and (d) thickness in layer 2. Note that the thickness gradient is dimensionless.

PV closure does not work well in our study. The flux–gradient relations become much noisier for PV than for thickness, which is not that well homogenized in some regions as is PV. This could give rise to the apparent paradox that, although eddy fluxes may be weak and very loosely constrained by mean flow gradients in homogenized regions, to obtain this homogenization one needs much larger and strongly constrained eddy fluxes. For instance, to obtain nearly uniform PV fields in a non-eddy-resolving model PV closure might work better than a thickness closure, although once nearly uniform PV fields have been obtained, a thickness closure better

simulates the divergent eddy fluxes than a PV closure. The extent to which parameterizations in eddy less models that are based on eddy flux relations in eddy-resolving models drive the mean states in the former models toward those of the eddy-resolving models is still largely untested. We do not test the skill of eddy parameterizations here, but we will pursue this issue in a following paper.

To elucidate the reasons why the eddy flux of PV in some regions is rather well correlated with the mean gradient of PV, but in other regions less well and also much worse than the linear correlation between the eddy flux of thickness and the mean gradient of thickness, we have to analyze the budgets of Eqs.(12) and (14). Often it is assumed that wind forcing in the upper layer complicates a downgradient eddy flux of PV and that only subsurface layers should be investigated in this respect. Equation (12) shows that this is not the case. Only the variable part of the forcing, and then only that part that is correlated with the eddy variability itself, affects the downgradient eddy flux of PV. The upper-layer wind forcing constrains the flow to cross PV contours also in the absence of significant eddy fluxes, but it does not affect the downgradient character of these fluxes themselves. The upper-layer PV balance of the present model consists of an approximate balance between eddy fluxes and advection by the mean flow, with the wind forcing playing a lesser important role (not shown). Here, mainly the eddy fluxes constrain the flow to cross PV contours.

Equation (12) is based on the assumption of a nondivergent velocity field, which holds in z coordinate models but not in isopycnic coordinate models. Accordingly, we have to rewrite Eq. (12) to be consistent with the model equations. In the present model this becomes

$$\overline{q'\nabla\cdot\mathbf{u}'\overline{q}} = -\overline{D'_q q'} - \overline{F'_q q'} - \frac{\nabla\cdot\overline{\mathbf{u}}\,\overline{q'^2}}{2} - \frac{\nabla\cdot\overline{\mathbf{u}'q'^2}}{2}, \tag{24}$$

which we rewrite as

$$\overline{\mathbf{u}'q'}\cdot\nabla\overline{q} = -\frac{\nabla\cdot\overline{\mathbf{u}}\,\overline{q'^2}}{2} - \frac{\nabla\cdot\overline{\mathbf{u}'q'^2}}{2} - \overline{D'_q q'} - \overline{F'_q q'} - \overline{q}\,\overline{q'\nabla\cdot\mathbf{u}'}. \tag{25}$$

Note that Eq. (25) now contains the term $-\overline{qq'\nabla\cdot\mathbf{u}'}$, which is zero in z coordinate models because $\overline{\mathbf{u}}$ and $\mathbf{u}'$ are nondivergent. Equation (25) is consistent with the balance in Eq. (13) when the rhs is dominated by $\overline{D'_q q'}$. In Fig. 15 the last three terms of the rhs of Eq. (25) are denoted as ''rest.''

Figure 15 shows that the main balance in the eddy enstrophy equation is not in agreement with Eq. (13). Apparently, the two-scale approximation invoked to arrive at this equation is not valid. In general, when the eddy fluxes are large, γ_q also becomes large. Largest eddy fluxes are found where the PV field quickly varies in space and time. In that case both particle displacements become large and the scale of variation of the PV field becomes small. Then, γ_q, the ratio between the two, quickly becomes large, that is, $O(1)$, and the advection of perturbation enstrophy cannot be neglected in Eq. (24). Also, when the fluxes are very small, Eq. (13) does not hold. In that case γ_q is small, say $O(\epsilon)$, but as the weak eddy fluxes are associated with weak PV gradients, either because PV is homogenized within a gyre or because the PV gradient is dominated by planetary vorticity, their product and all other terms in Eq. (24) become of $O(\epsilon)$, and again the advection of perturbation enstrophy cannot be neglected.

Figure 15 shows that, although the zonally averaged eddy PV flux is downgradient almost everywhere, the advection of perturbation enstrophy is a first-order quantity. Moreover, it has a multisigned character and does not scale well with mean-flow gradients. As a result, locally the eddy PV flux is less well related to mean-flow gradients and features larger areas of upgradient transport than suggested by the balance of Eq. (13). Only in the flow regime where PV gradients are modestly weak/large the balance of Eq. (13) holds, and a diffusive closure for the eddy flux of PV is valid. Rhines and Holland (1979) argue that the restriction that γ_q is small is more easily satisfied for parallel flow than for curved flow, as in the latter case particle displacements from their rest latitude can be large, even when the eddy displacements themselves are small. Therefore, for a reentrant channel flow the regime for which Eq. (13) holds is much larger than for a closed basin double-gyre flow, and subsequently, a diffusive closure for the eddy PV flux works much better. This, at least partly, explains the discrepancy between our results and those of Lee et al. (1997), Killworth (1998), and Treguier (1999). It should be noted that Marshall and Shuts (1981) attempted to account for curvature and argued that a redefined eddy flux is still downgradient. However, if γ_q becomes large due to curvature, the eddy diffusivity becomes a function of curvature and the relation between eddy fluxes and mean flow gradients becomes obscure.

Unlike PV, layer thickness is not conserved and a balance like Eq. (13) never holds for the variance of perturbation thickness. There always is an additional forcing by vertical motions; $-\overline{w'h'}$; see Eq. (15). This forcing term, however, acts in most cases to dissipate thickness variance (Fig. 16), as it is dominated by the conversion from potential to kinetic energy that results from baroclinic instability and the subsequent downgradient transport of heat and layer thickness. In the middle layer this is not the case, but there the advection of perturbation thickness variance secures the downgradient transport of the eddy thickness flux. Apart from the middle layer where the flow is weakest, γ_h appears to be smaller than γ_q, reflected by a less important role of advection of thickness variance compared to advec-

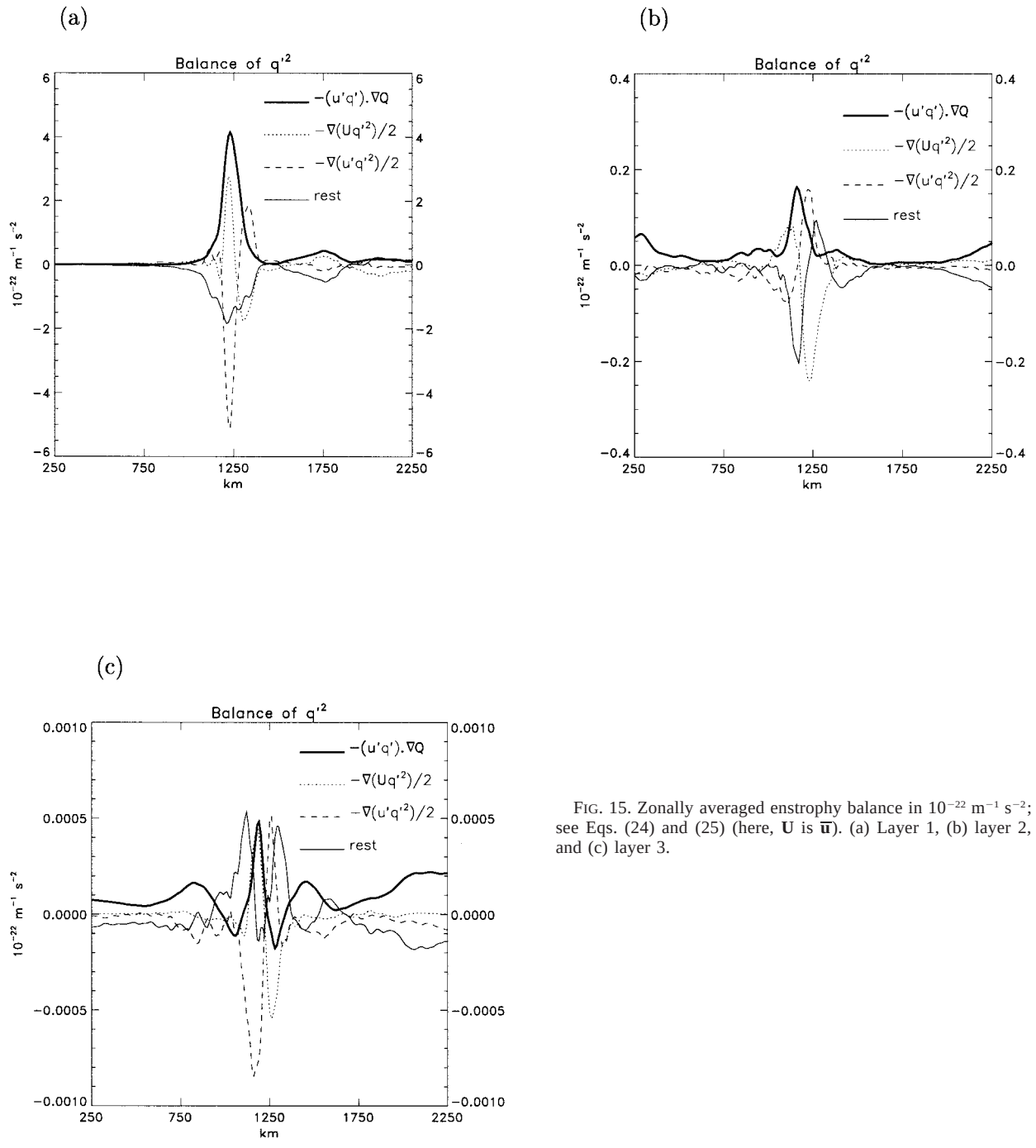

FIG. 15. Zonally averaged enstrophy balance in 10^{-22} m^{-1} s^{-2}; see Eqs. (24) and (25) (here, **U** is $\overline{\mathbf{u}}$). (a) Layer 1, (b) layer 2, and (c) layer 3.

tion of enstrophy. Also, the advection of perturbation thickness variance is more single signed and mean flow related than the advection of perturbation enstrophy, which is mainly caused by the relative vorticity contribution to the latter. As a result, the downgradient diffusive closure for layer thickness appears to simulate the divergent eddy fluxes better than a downgradient diffusive closure for PV in the double-gyre flow considered here.

A cautionary remark should be made when discussing closure relations for the bolus transport within an isopycnic model. Such a closure is not always straightforwardly translated into a closure for a *z* coordinate model. Within a *z* coordinate model the definition for the bolus velocity becomes $u_* = (\overline{\mathbf{u}'\rho'}/\overline{\rho}_z)_z$ instead of $\mathbf{u}_* = \overline{\mathbf{u}'h'}/\overline{h}$. Now, advection of density by the sum of the Eulerian mean and bolus velocity does not strictly conserve density as layer thickness, where mass flux di-

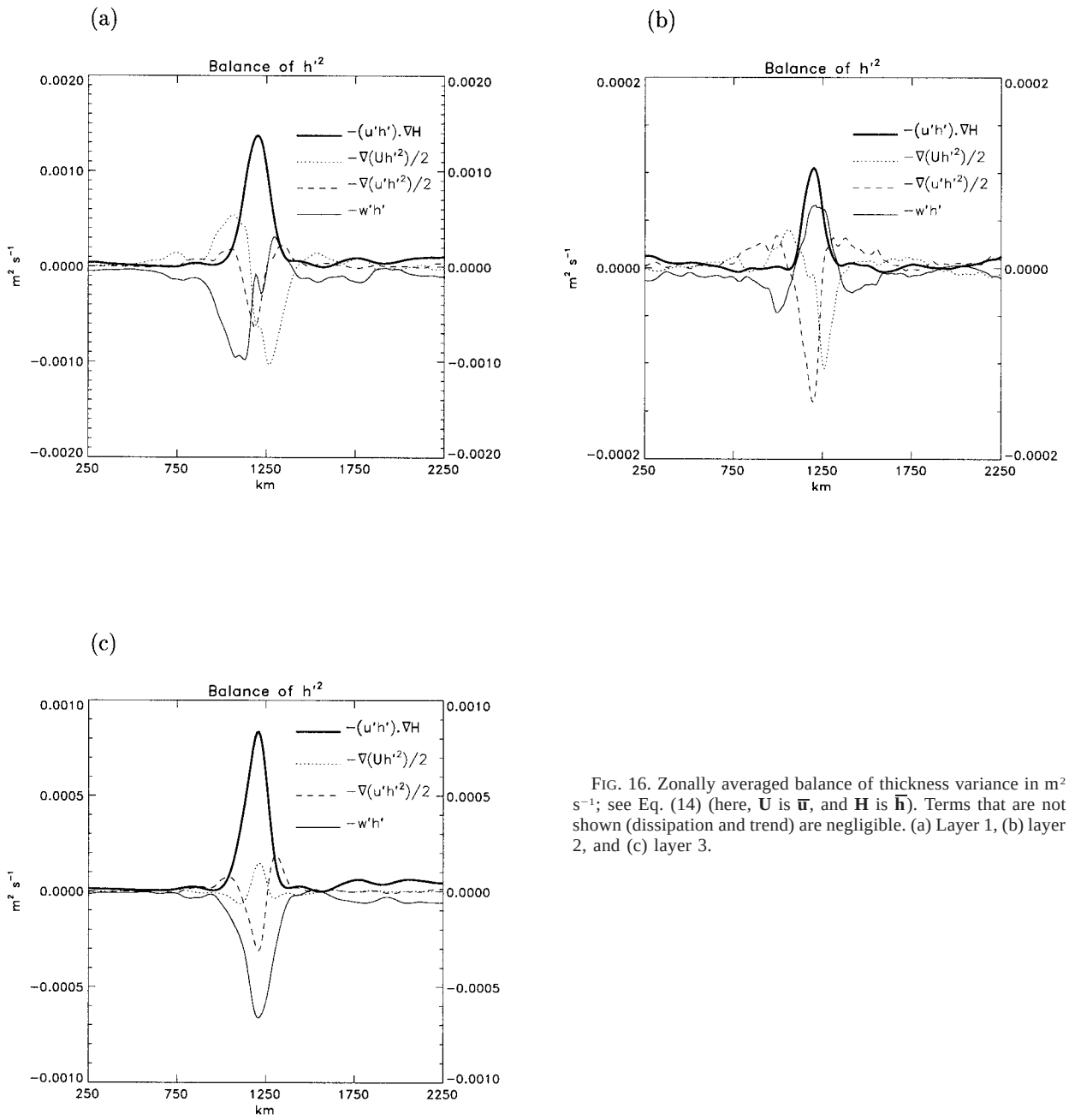

FIG. 16. Zonally averaged balance of thickness variance in m^2 s^{-1}; see Eq. (14) (here, **U** is $\overline{\mathbf{u}}$, and **H** is $\overline{\mathbf{h}}$). Terms that are not shown (dissipation and trend) are negligible. (a) Layer 1, (b) layer 2, and (c) layer 3.

vergences are calculated from the sum of the Eulerian mean and bolus velocity. A forcing term enters the density equation of the form $(\overline{\mathbf{u}'\rho'} \cdot \nabla\overline{\rho}/\overline{\rho}_z)_z$. When the downgradient eddy flux of density is small, in the equation for perturbation density variance [Eqs. (12) or (24), with q replaced by ρ] this term is primarily balanced by dissipation; that is, for perturbation density variance a balance like Eq. (13) holds. In that case, the forcing of the density equation can be neglected as eddy density fluxes primarily act along density surfaces. It is on this assumption that the Gent and McWilliams parameterization is based.

McDougall and McIntosh (1996) and McDougall (1998) argue that a balance like Eq. (13) does not hold for perturbation density variance and that the advection of density variance by the mean flow has to be included in this balance. In that case, a transformed residual mean velocity can be defined that consists of the sum of the Eulerian mean flow, the bolus velocity, and an extra term that negates the influence of the advection of density variance. Now, density is conserved when advected with the transformed residual mean velocity up to third order in perturbation amplitude. However, Gille and Davis (1999) notice that in their model simulations of both

the Eady problem and a wind-driven reentrant channel, self-advection of perturbation density variance becomes a first-order quantity. This implies that the perturbation amplitude becomes large and that density is not conserved when advected by the transformed residual mean velocity. Although we do not carry a prognostic equation for density in our isopycnic model the equation for the perturbation density variance is equivalent to the equation for thickness variance when the terms $\overline{\mathbf{u}'h'} \cdot \nabla\overline{h}$ and $\overline{w'h'}$ in Eq. (14) are taken together. We see from Fig. 16 that, in general, advection of thickness variance by the mean flow dominates dissipation, so the extension of McDougall and McIntosh (1996) and McDougall (1998) to the Gent and McWilliams parameterization is important, if not essential. However, in most cases self advection of thickness variance becomes as important as advection of thickness variance by the mean flow, consistent with the findings of Gille and Davies (1999), and the parameterization of McDougall (1998) has to be extended to account for this.

7. Conclusions

We have investigated eddy fluxes of PV and laver thickness in an idealized isopycnic eddy-resolving ocean model with a high horizontal resolution (10 km) and low vertical resolution (three layers). The model simulates a wind-driven double-gyre flow within a flat bottom, closed basin. Variations in upper-layer depth were of $O(1)$, but outcropping did not occur. Fluxes have been decomposed into divergent and rotational parts and only the divergent contribution was examined. In this study we have not tested the skill of certain parameterizations but discussed the rationalization of PV and thickness closures in the present configuration. We found the following features:

1) The divergent eddy PV flux tends to be of smaller scale signature than the divergent eddy thickness flux. Both are dominated by large values near the separation of the midlatitude jet. The relative vorticity contribution to the eddy PV flux becomes important here, which causes the smaller scales to become more dominant.

2) The eddy diffusivity for both thickness and PV yields negative values in the eastern part of the midlatitude jet and in the center of the tight recirculation cells, where eddies decay. Everywhere else they are positive. The eddy diffusivity for PV is noisier, and the regions with a negative diffusivity are larger.

3) The zonally averaged eddy flux of thickness scales better with the zonally averaged meridional thickness gradient than the eddy flux of PV with the PV gradient, especially near the midlatitude jet where the relative vorticity contribution to the latter becomes important. The amplitude of the inversely derived eddy diffusivity varies greatly, both in the horizontal and vertical.

4) When the mean PV gradient is either not too weak or not too strong, a diffusive closure for PV can work better than for thickness. If it is too weak, the flux–gradient relation for PV becomes too noisy compared to thickness, which generally is less well homogenized. If the PV gradient is too strong, the role of relative vorticity in the eddy PV fluxes becomes important and the flux–gradient relation is flawed.

5) Advection of perturbation enstrophy generally disturbs the balance between the cross-gradient eddy flux of PV and dissipation on which the diffusive closure is based. When the flow is strong, curvature, a mean field scaling with the jet width, and large-scale meandering makes this term of $O(1)$. When the flow is weak, homogenization of PV makes the first-order terms small and curvature enhances the higher order terms. All terms become of equal importance: $O(\epsilon)$.

6) Forcing by vertical motions in most cases acts to dissipate thickness variance, as it is dominated by the conversion from potential to kinetic energy and the subsequent downgradient transport of thickness. In addition, advection of perturbation thickness variance is more simply related to mean flow gradients than advection of perturbation enstrophy. As a result, in the present configuration a downgradient diffusive closure for thickness seems more appropriate to simulate the divergent eddy fluxes than a downgradient diffusive closure for PV, especially in dynamically active regions where the eddy fluxes are large and in regions where PV is nearly uniform.

REFERENCES

Andrews, D. G., and M. E. McIntyre, 1976: Planetary waves in horizontal and vertical shear: The generalized Eliassen–Palm relation and the zonal mean acceleration. *J. Atmos. Sci.,* **33,** 2031–2048.

———, T. R. Holton, and C. B. Leovy, 1987: *Middle Atmosphere Dynamics.* Academic Press, 489 pp.

Bleck, R., and D. B. Boudra, 1981: Initial testing of a numerical ocean circulation model using a hybrid (quasi-isopycnic) vertical coordinate. *J. Phys. Oceanogr.,* **11,** 755–770.

——, and ——, 1986: Wind driven spin-up in eddy-resolving ocean models formulated in isopycnic and isobaric coordinates. *J. Geophys. Res.,* **91,** 7611–7621.

Bryan, K., J. K. Dukowicz, and R. D. Smith, 1999: On the mixing coefficient in the parameterization of bolus velocity. *J. Phys. Oceanogr.,* **29,** 2442–2456.

Danabasoglu, G., and J. C. McWilliams, 1995: Sensitivity of the global ocean circulation to parameterizations of mesoscale tracer transports. *J. Climate,* **8,** 2967–2987.

Drijfhout, S. S., 1994: On the heat transport by mesoscale eddies in an ocean circulation model. *J. Phys. Oceanogr.,* **24,** 429–442.

Duffy, P. B., P. Eltgroth, A. J. Bourgeois, and K. Caldeira, 1995: Effect of improved subgrid scale transport of tracers on uptake of bomb radiocarbon in the GFDL ocean general circulation model. *Geophys. Res. Lett.,* **22,** 1065–1068.

England, M. H., 1995: Using chlorofluorocarbons to assess ocean climate models. *Geophys. Res. Lett.,* **22,** 3051–3054.

Gent, P. R., and J. C. McWilliams, 1990: Isopycnic mixing in ocean circulation models. *J. Phys. Oceanogr.,* **20,** 150–155.

——, J. Willebrand, T. J. McDougall, and J. C. McWilliams, 1995: Parameterizing eddy-induced tracer transports in ocean circulation models. *J. Phys. Oceanogr.,* **25,** 463–474.

Gille, S. T., and R. E. Davis, 1999: The influence of mesoscale eddies on coarsely resolved density: An examination of subgrid-scale parameterization. *J. Phys. Oceanogr.,* **29,** 1109–1123.

Greatbatch, R. J., 1998: Exploring the relationship between eddy-induced transport velocity, vertical momentum transfer, and the isopycnal flux of potential vorticity. *J. Phys. Oceanogr.,* **28,** 422–432.

Hirst, A. C., and T. J. McDougall, 1996: Deep-water properties and surface buoyancy flux as simulated by a *z* coordinate model including eddy-induced advection. *J. Phys. Oceanogr.,* **26,** 1320–1343.

Holland, W. R., and P. B. Rhines, 1980: An example of eddy-induced ocean circulation. *J. Phys. Oceanogr.,* **10,** 1010–1031.

——, T. Keffer, and P. B. Rhines, 1984: Dynamics of the oceanic general circulation: The potential vorticity field. *Nature,* **308,** 698–705.

Jiang, S., F.-F. Jin, and M. Ghil, 1995: Multiple equilibria, periodic and aperiodic solutions in a wind-driven, double-gyre, shallow-water model. *J. Phys. Oceanogr.,* **25,** 764–786.

Killworth, P. D., 1997: On the parameterization of eddy transfer. Part I: Theory. *J. Mar. Res.,* **55,** 1171–1197.

——, 1998: On the parameterization of eddy transfer. Part II: Tests with a channel model. *J. Mar. Res.,* **56,** 349–374.

Lee, M.-M., D. P. Marshall, and R. G. Williams, 1997: On the eddy transfer of tracers: Advective or diffusive? *J. Mar. Res.,* **55,** 483–505.

Marshall, D. P., R. G. Williams, and M.-M. Lee, 1999: The relation between eddy-induced transport and isopycnic gradients of potential vorticity. *J. Phys. Oceanogr.,* **29,** 1571–1578.

Marshall, J. C., and G. Shutts, 1981: A note on rotational and divergent eddy fluxes. *J. Phys. Oceanogr.,* **11,** 1677–1680.

McDougall, T. J., 1998: Three-dimensional residual-mean theory. *Ocean Modeling and Parameterization,* E. P. Chassignet and J. Verron, Eds., NATO ASI Series C, Kluwer Academic, 95–122.

——, and P. C. McIntosh, 1996: The temporal-residual-mean velocity. Part I: Derivation and the scalar conservation equations. *J. Phys. Oceanogr.,* **26,** 2653–2665.

McDowell, S., P. B. Rhines, and T. Keffer, 1982: North Atlantic potential vorticity and its relation to the general circulation. *J. Phys. Oceanogr.,* **12,** 1417–1436.

McWilliams, J. C., W. R. Holland, and J. H. S. Chow, 1978: A description of numerical Antarctic Circumpolar Currents. *Dyn. Atmos. Oceans,* **2,** 213–291.

O'Dwyer, J., and R. G. Williams, 1997: The climatological distribution of potential vorticity over the abyssal ocean. *J. Phys. Oceanogr.,* **27,** 2488–2506.

Plumb, R. A., and J. D. Mahlman, 1987: The zonally-averaged transport characteristics of the GFDL General Circulation/Transport Model. *J. Atmos. Sci.,* **44,** 298–327.

Press, W. H., B. P. Flannery, S. A. Teukolsky, and W. T. Vetterling, 1986: *Numerical Recipes: The Art of Scientific Computing.* Cambridge University Press, 818 pp.

Rhines, P. B., 1977: The dynamics of unsteady currents. *The Sea.* Vol 6: *Marine Modelling,* E. Goldberg, Ed., Wiley, 189–318.

——, and W. R. Holland, 1979: A theoretical discussion of eddy-driven flows. *Dyn. Atmos. Oceans,* **3,** 289–325.

Rix, N. H., and J. Willebrand, 1996: Parameterization of mesoscale eddies as inferred from a high-resolution circulation model. *J. Phys. Oceanogr.,* **26,** 2281–2285.

Schmitz, W. J., 1977: On the deep general circulation in the western North Atlantic. *J. Mar. Res.,* **35,** 21–28.

Smagorinsky, J. S., 1963: General circulation experiments with the primitive equations. I: The basic experiment. *Mon. Wea. Rev.,* **91,** 99–164.

Stammer, D., 1998: On eddy characteristics, eddy transports, and mean flow properties. *J. Phys. Oceanogr.,* **28,** 727–739.

Treguier, A. M., 1999: Evaluating eddy mixing coefficients from eddy-resolving ocean models: A case study. *J. Mar. Res.,* **57,** 89–108.

——, I. Held, and V. Larichev, 1997: On the parameterization of quasi-geostrophic eddies in primitive equation ocean models. *J. Phys. Oceanogr.,* **27,** 567–580.

Visbeck, M., J. Marshall, and T. Haine, 1997: Specification of eddy transfer coefficients in coarse-resolution ocean circulation models. *J. Phys. Oceanogr.,* **27,** 381–402.

Wunsch, C., 1999: Where do ocean eddy heat fluxes matter? *J. Geophys. Res.,* **104,** 13 235–13 249.